

FTIR ANALYSIS OF LASER SHOCKED SILICON

THESIS

Presented to the Graduate Council of  
Texas State University-San Marcos  
in Partial Fulfillment  
of the Requirements

for the Degree

Master of SCIENCE

by

Dominic Chiroro, B.S., M.S.

San Marcos, Texas

May, 2012

**COPYRIGHT**

by

Dominic Chiroro

2012

## **FAIR USE AND AUTHOR'S PERMISSION STATEMENT**

### **Fair Use**

This work is protected by the Copyright Laws of the United States (Public Law 94-553, Section 107). Consistent with fair use as defined in the Copyright Laws, brief quotations from this material are allowed with proper acknowledgement. Use of this material for financial gain without the author's express written permission is not allowed.

### **Duplication Permission**

As the copyright holder of this work I, Dominic Chiroro, authorize duplication of this work in whole or in part, for educational or scholarly purposes only.

## ACKNOWLEDGEMENTS

Many people helped me in various ways to successfully complete my studies at Texas State. I am grateful to my advisor Dr. Donnelly for initiating the research and for providing guidance throughout the course of the research. I learnt a great deal from interacting with him. I would also like to thank Dr. Anup Bandyopadhyay for helping me to clean the samples which I used in the research. I thank all the people and organizations which gave me support during my studies. Special mention goes to Dr. Terry Golding and my friend Dr. Tom Hopson. I am extremely grateful for the support which you gave me. I could not have made it without it. The Physics department at Texas State deserves special mention as well for funding my studies. I am most grateful for the support which I got. I thank my friends Peter Heinz and Amanda Gregory for helping me with books. Lastly, I would like to thank my wife Tendai for her patience as I spent many nights away from home while conducting experiments in the laboratory. It is to her that this thesis is dedicated!

This manuscript was submitted on 5 April 2012.

## TABLE OF CONTENTS

	<b>Page</b>
ACKNOWLEDGEMENTS .....	v
TABLE OF CONTENTS.....	vi
LIST OF TABLES .....	viii
LIST OF FIGURES .....	ix
CHAPTER	
I. INTRODUCTION .....	1
Background.....	1
Structure of the Thesis.....	3
II. LITERATURE REVIEW .....	5
Introduction .....	5
Energy Levels in Silicon.....	6
Effective Mass Theory.....	13
Spectra due to Acceptors .....	19
III. METHODS AND MATERIALS .....	23
Introduction .....	23
Sample Preparation.....	23
Sample Analysis .....	24
Room Temperature Measurements.....	24
Liquid Helium Temperature Measurements.....	26
IV. RESULTS AND DISCUSSION .....	27
Introduction .....	27

Room Temperature Measurements.....	27
Liquid Helium Temperature Measurements.....	29
V. CONCLUSIONS AND RECOMMENDATIONS.....	56
Introduction .....	56
Conclusions .....	56
Recommendations for Further Research .....	57
REFERENCES .....	58

## LIST OF TABLES

<b>Table</b>	<b>Page</b>
Table 1: Binding energies of some energy levels of substitutional phosphorus in silicon (meV).....	17
Table 2: Position ( $\text{cm}^{-1}$ ) of some of the electronic excitation lines of boron in silicon (after Pajot and Debarre 1981). ....	22
Table 3: Observed peaks ( $\text{cm}^{-1}$ ) for samples from wafer 1.....	28
Table 4: Observed peaks ( $\text{cm}^{-1}$ ) for samples from wafer 2.....	29
Table 5: Observed electronic excitation lines ( $\text{cm}^{-1}$ ) for samples from wafer 1.....	30
Table 6: Observed electronic excitation lines ( $\text{cm}^{-1}$ ) for samples from wafer 2.....	31

## LIST OF FIGURES

<b>Figure</b>	<b>Page</b>
Figure 1: Formation of energy bands as a diamond lattice crystal is formed by bringing isolated silicon atoms together (after Sze 2002).....	7
Figure 2: Creation of electron-hole pairs in a semiconductor (after Streetman and Banerjee, 2002).....	8
Figure 3: Donor level filled with electrons at 0 K (after Streetman and Banerjee, 2002).	10
Figure 4: Donation of electrons from donor level to conduction band (after Streetman and Banerjee, 2002).....	10
Figure 5: Acceptor level empty of electrons at 0 K (after Streetman and Banerjee, 2002). .....	11
Figure 6: Acceptance of valence band electrons by an acceptor level and creation of holes in the valence band (after Streetman and Banerjee, 2002). ....	12
Figure 7: Excitation spectrum of phosphorus donors in silicon doped with phosphorus at liquid helium temperature (after Jagannath <i>et al.</i> 1981).....	16
Figure 8: Energy level scheme of group V impurities in silicon for transitions from the 1s states to the 2p <sub>0</sub> , 2p <sub>±</sub> states (after Ramdas and Rogriguez 1981).....	19
Figure 9: The spin-orbit-split valence band of silicon with associated states. Here GS is the ground state and $\lambda$ is the spin-orbit splitting at $k = 0$ (after Ramdas and Rogriguez 1981). ....	20
Figure 10: Excitation spectrum of silicon doped with boron.....	21
Figure 11: Spectrum for sample 1 of wafer 1, trial 1.....	32
Figure 12: Spectrum for sample 1 of wafer 1, trial 2.....	33
Figure 13: Spectrum for sample 2 of wafer 1, trial 1.....	34

Figure 14: Spectrum for sample 2 of wafer 1, trial 2.....	35
Figure 15: Spectrum for sample 3 of wafer 1, trial 1.....	36
Figure 16: Spectrum for sample 3 of wafer 1, trial 2.....	37
Figure 17: Spectrum for sample 1 of wafer 2, trial 1.....	38
Figure 18: Spectrum for sample 1 of wafer 2, trial 2.....	39
Figure 19: Spectrum for sample 2 of wafer 2, trial 1.....	40
Figure 20: Spectrum for sample 2 of wafer 2, trial 2.....	41
Figure 21: Spectrum for sample 3 of wafer 2, trial 1.....	42
Figure 22: Spectrum for sample 3 of wafer 2, trial 2.....	43
Figure 23: Spectrum for sample 1 of wafer 1, trial 1.....	44
Figure 24: Spectrum for sample 1 of wafer 1, trial 2.....	45
Figure 25: Spectrum for sample 2 of wafer 1, trial 1.....	46
Figure 26: Spectrum for sample 2 of wafer 1, trial 2.....	47
Figure 27: Spectrum for sample 3 of wafer 1, trial 1.....	48
Figure 28: Spectrum for sample 3 of wafer 1, trial 2.....	49
Figure 29: Spectrum for sample 1 of wafer 2, trial 1.....	50
Figure 30: Spectrum for sample 1 of wafer 2, trial 2.....	51
Figure 31: Spectrum for sample 2 of wafer 2, trial 1.....	52
Figure 32: Spectrum for sample 2 of wafer 2, trial 2.....	53
Figure 33: Spectrum for sample 3 of wafer 2, trial 1.....	54
Figure 34: Spectrum for sample 3 of wafer 2, trial 2.....	55

## CHAPTER I

### INTRODUCTION

#### Background

The electrical properties of a semiconductor can be altered by adding controlled amounts of appropriate impurities to the semiconductor. These impurities are called dopants and for silicon they are trivalent or pentavalent atoms. For the impurity atoms to be electrically active they should occupy lattice positions normally occupied by the host atoms. These positions are referred to as substitutional positions. Any other positions in the crystal lattice are referred to as interstitial positions. The impurities can be added to the semiconductor in several ways. One of these methods is ion implantation. In this process a beam of ions is accelerated to high energies and is directed onto the surface of the semiconductor (Streetman and Banerjee, 2002). During the implantation process ions can knock atoms out of their lattice positions thereby damaging the implanted region (Jaegar, 2002). In addition, some of the implanted ions come to rest in the crystal lattice at interstitial positions rather than at substitutional positions. The implantation damage can be removed by an annealing step. This can be done by heating the implanted material at a high temperature. This process is called thermal annealing. Typically for silicon the wafer is heated at a temperature between 800 and 1000°C for a period of about 30

minutes (Jaegar, 2002). During the annealing process the host atoms move back into lattice positions and the impurity atoms move into substitutional positions (Jaegar, 2002). The impurity atoms become electrically active when they move to substitutional positions.

Unfortunately, thermal annealing leads to unintended diffusion of the dopants (Campbell, 2008). This diffusion can be minimized by optimizing the annealing time and temperature (Streetman and Banerjee, 2002). Rapid thermal annealing is an example of a technique which can be used to achieve this. Another method which could be used to minimize unintended diffusion is athermal annealing (Donnelly *et al.*, 1997). In this method, the material to be annealed is irradiated with a pulse of a high intensity laser beam. Research has shown that annealing takes place in the region well beyond the spot on which the laser beam is directed (Grun *et al.*, 1997; Donnelly *et al.*, 1997; Grun *et al.*, 2000a). For example Donnelly *et al.* (1997) demonstrated this using 25 x 25 x 2 mm Si samples. The samples were doped with phosphorus to a concentration of about  $10^{15} \text{ cm}^{-3}$ . Some of the samples were then irradiated with one or two pulses from the PHAROS III laser ( $\lambda = 1.06 \text{ }\mu\text{m}$ ,  $t = 5 \text{ ns}$  and  $E \sim 10 \text{ J}$ ). The laser pulses were focused to a spot 1 mm in diameter on the surface of the sample. Four-point probe measurements on the front and back of the wafer gave the same value for sheet resistance suggesting that the laser irradiation focused in the center produced uniform n-type activation over the entire sample. Similar results were obtained for boron-doped silicon when it was annealed athermally (Donnelly *et al.*, 2001). The annealing produced by the athermal technique is comparable to that which can be attained by thermal annealing. Furthermore

this technique results in much less unintended diffusion as compared to thermal annealing (Grun *et al.*, 2000b; Donnelly *et al.*, 2001). This makes this technique attractive to use for the production of the next-generation ultra-high density devices since it minimizes unintended diffusion which can degrade the definition of features (Grun *et al.*, 1997).

Research by Grun *et al.* (2000a) suggests that heat from the laser is not responsible for annealing the samples. They speculate that shock waves are responsible for the annealing that is observed. They suggest that when the sample is illuminated with the laser at high intensities, a plasma is generated which then creates high-pressure shock waves within the surrounding solid. The pressure waves and accompanying rarefaction waves reverberate within the sample for tens of microseconds (Grun *et al.*, 2000a).

Since athermal annealing takes place beyond the region on which the laser pulse is directed it seems reasonable that if a large sample is irradiated with a laser beam at a number of points then this might result in the whole sample being annealed. The objective of this research is to determine if athermal annealing could be effective in annealing a whole wafer rather than just parts of it. If this is possible then this would make the technique more useful from a practical perspective.

### Structure of the Thesis

The thesis is divided into five chapters. The first chapter gives background information concerning the research. Chapter two gives the theory behind the techniques used in the research. In chapter three the materials and methods used in the research are presented. In

chapter four the results obtained in the research are presented and analyzed. Finally, chapter five gives the conclusions and the recommendations for further research.

## CHAPTER II

### LITERATURE REVIEW

#### Introduction

This research involved the analysis of silicon wafers which were subjected to single laser pulses at a number of points. The objective of the research was to determine the effectiveness of the technique in annealing the whole wafer. This was achieved by conducting far infrared absorption studies on samples from the wafers using a Fourier Transform infrared (FT-IR) spectrometer (Grun *et al.*, 1997; Donnelly *et al.*, 1997). Research has shown that if phosphorus-doped silicon is annealed, that is, dopant atoms are electrically active, it produces hydrogen-like spectra when irradiated with infrared radiation at low temperatures (Kohn, 1957a; Ramdas and Rodriguez, 1981; Mayur *et al.*, 1993; Lynch *et al.*, 2010). The presence or absence of the spectra can thus be used to determine whether a sample has been annealed or not ((Grun *et al.*, 1997; Donnelly *et al.*, 1997). This chapter gives the theory behind the experimental techniques which were used in the research.

### Energy Levels in Silicon

In contrast to the discrete energy levels in single atoms, solids have bands of very closely spaced energy levels which are available for occupation by electrons (Kittel, 1986).

Consecutive bands of allowed energy levels are separated by regions of energies which the electrons are not allowed to take. The energy levels are filled by electrons starting with the lower energy levels. The two highest bands, the valence band and the conduction band, as well as the size of the energy gap between them play a crucial role in determining the physical properties of a solid (Wilson and Hawkes, 1989).

The electronic configuration of a silicon atom in the ground state is  $1s^2 2s^2 2p^6 3s^2 3p^2$ . It has four valence electrons. Consider  $N$  silicon atoms which are a large distance apart. The total number of valence electrons is  $4N$ . The number of  $3s$  and  $3p$  states available for occupation by these valence electrons is  $2N$  and  $6N$  respectively. When silicon atoms are brought together to form a silicon crystal the  $3s$  and  $3p$  orbitals undergo  $sp^3$  hybridization (Streetman and Banerjee, 2002). The original  $8N$  states group into two energy bands separated by an energy gap with  $4N$  states in each band. The lower band is the valence band and the upper band is the conduction band. Figure 1 shows schematically the formation of the energy bands as a diamond lattice crystal is formed by bringing isolated silicon atoms together. At  $0\text{ K}$  electrons will occupy the lowest energy states available to them. In silicon the  $4N$  valence electrons occupy the  $4N$  energy states in the valence band thus filling up this band of energy states (Person and Bardeen, 1948; Streetman and Banerjee, 2002; Sze, 2002). The conduction band is therefore empty at  $0$

K. At temperatures above 0 K some electrons in the valence band acquire enough thermal energy to be excited across the band gap into the conduction band.

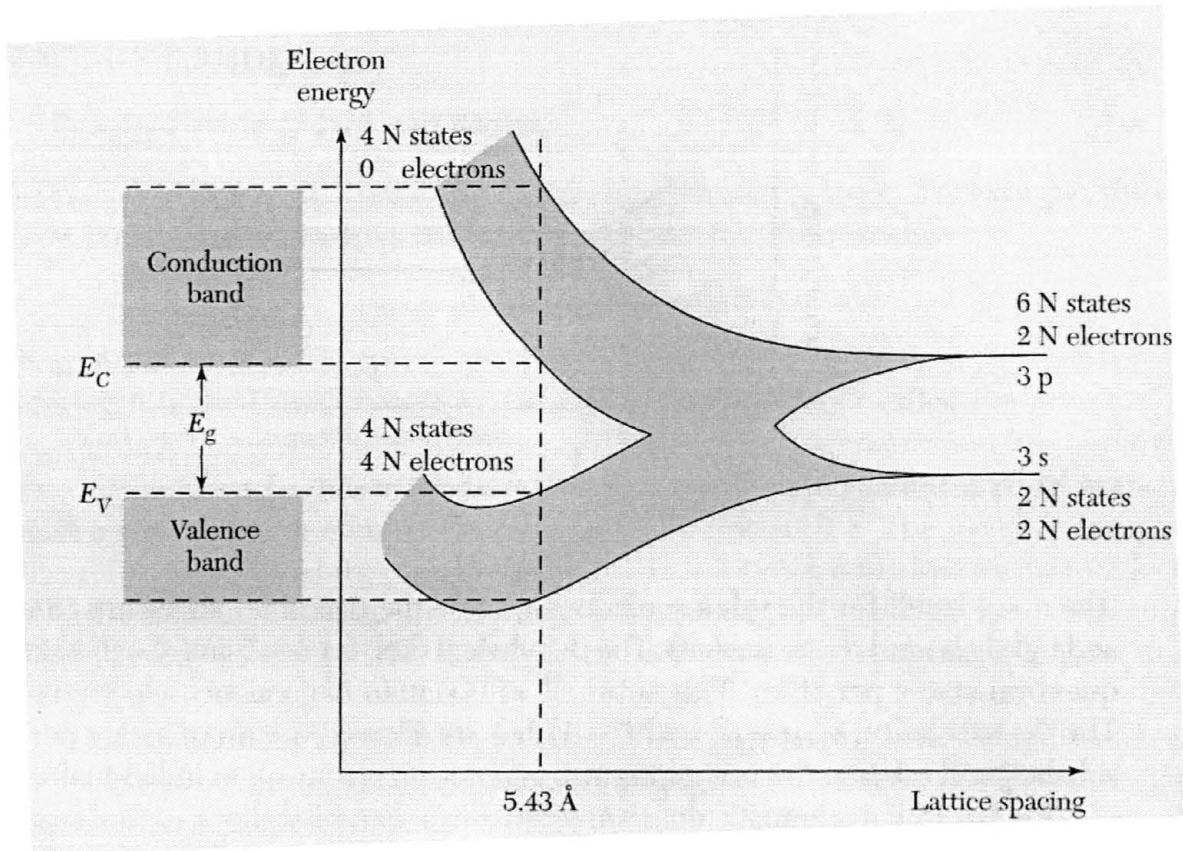


Figure 1: Formation of energy bands as a diamond lattice crystal is formed by bringing isolated silicon atoms together (after Sze 2002).

This process introduces electrons into the conduction band. Each electron which moves from the valence band to the conduction band leaves an empty state in the valence band. This is illustrated in figure 2. An empty state in the valence band is referred to as a hole. If the conduction band electron and the valence band hole are created by the excitation of

a valence band electron to the conduction band, they are called an electron-hole pair (Streetman and Banerjee, 2002).

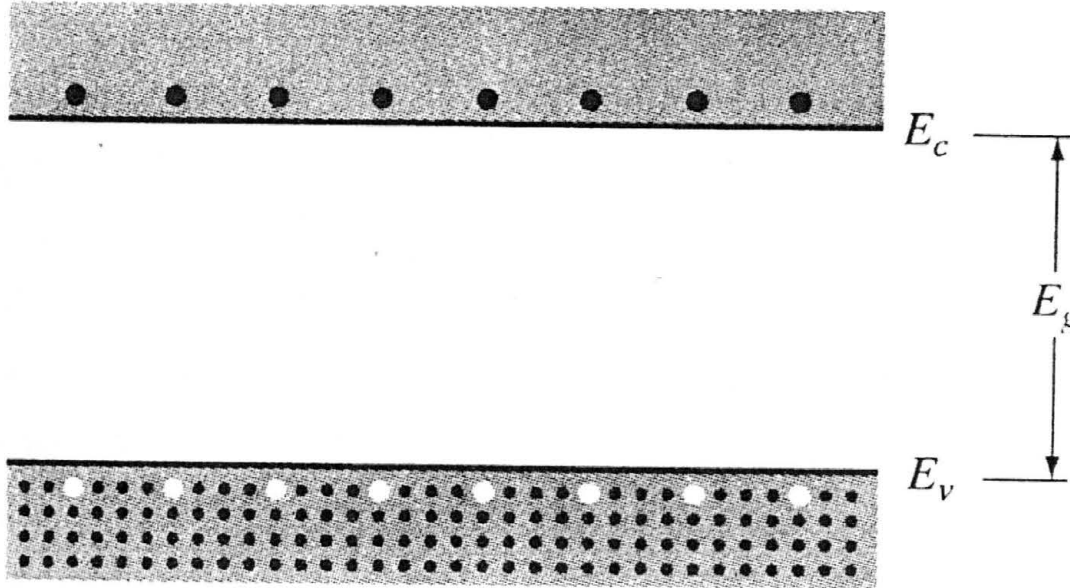


Figure 2: Creation of electron-hole pairs in a semiconductor (after Streetman and Banerjee, 2002).

The holes can be treated as charge carriers with positive charge and positive mass (Wilson and Hawkes, 1989; Streetman and Banerjee, 2002; Sze, 2002).

A perfect semiconductor with no impurities or lattice defects is called an intrinsic semiconductor. In such a material, there are no charge carriers at 0 K, since the valence band is filled with electrons and the conduction band is empty. At higher temperatures electron-hole pairs are generated as valence band electrons are excited thermally across

the band gap to the conduction band. As the carriers are generated in pairs the concentration  $n$  of electrons in the conduction band is equal to the concentration  $p$  of holes in the valence band (Wilson and Hawkes, 1989).

The number of charge carriers in a semiconductor can be vastly increased by introducing appropriate impurities into the crystal. This process is called doping. Through doping, a crystal can be altered so that it has a predominance of either electrons or holes. Thus there are two types of doped semiconductors, n-type (where the majority carriers are negative electrons and the minority carriers are holes) and p-type (where the majority carriers are positive holes). In doped semiconductors the carrier concentrations are no longer equal and the material is said to be extrinsic (Wilson and Hawkes, 1989).

When impurities or lattice defects are added to an otherwise perfect crystal, one or more discrete energy levels are introduced into the energy gap (Schroder, 1998; Streetman and Banerjee, 2002; Sze, 2002). An impurity from column V of the periodic table (P, As and Sb) has one more valence electron than silicon and thus introduces an energy level very near the conduction band in silicon. This level is filled with electrons at 0 K as shown in figure 3. Very little thermal or optical energy is required to excite these electrons to the conduction band.

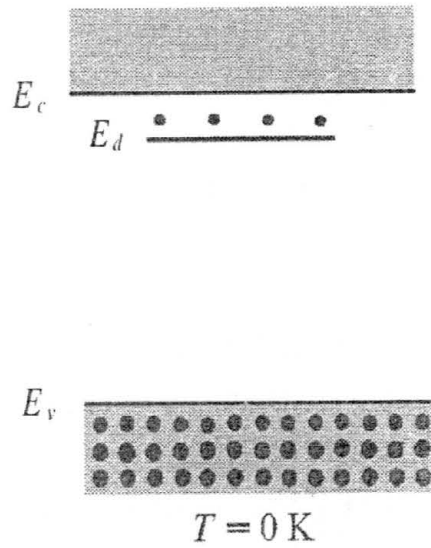


Figure 3: Donor level filled with electrons at 0 K (after Streetman and Banerjee, 2002).

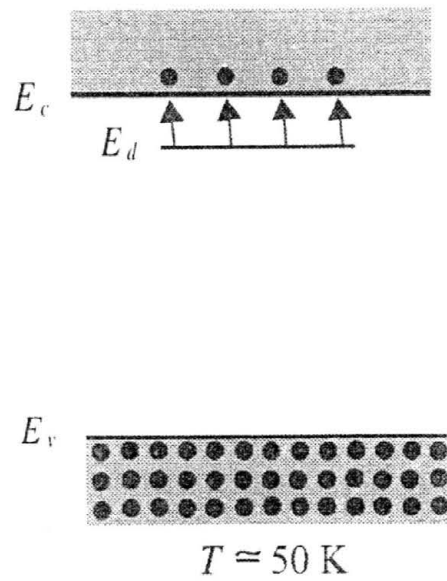


Figure 4: Donation of electrons from donor level to conduction band (after Streetman and Banerjee, 2002).

As  $E_c - E_d$  is typically 45 meV, at about 50-100 K virtually all the electrons in the impurity level are donated to the conduction band. This is illustrated in figure 4. Such an impurity level is called a donor level, and the column V impurities in silicon are called donor impurities since they donate electrons to the conduction band (Wilson and Hawkes, 1989; Streetman and Banerjee, 2002).

Atoms from column III (B, Al, Ga, and In) introduce impurity levels in Si near the valence band. As shown in figure 5, these levels are empty of electrons at 0 K. Very little thermal or optical energy is required to excite electrons from the valence band to the impurity levels.

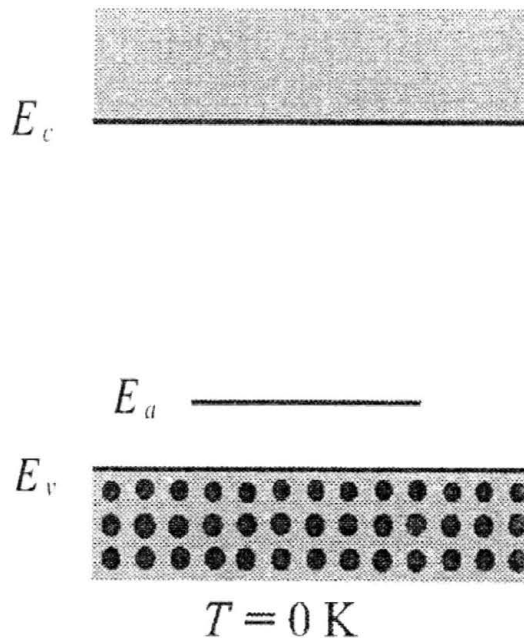


Figure 5: Acceptor level empty of electrons at 0 K (after Streetman and Banerjee, 2002).

When electrons in the valence band are excited to these impurity levels they leave behind holes in the valence band. This is shown in figure 6.

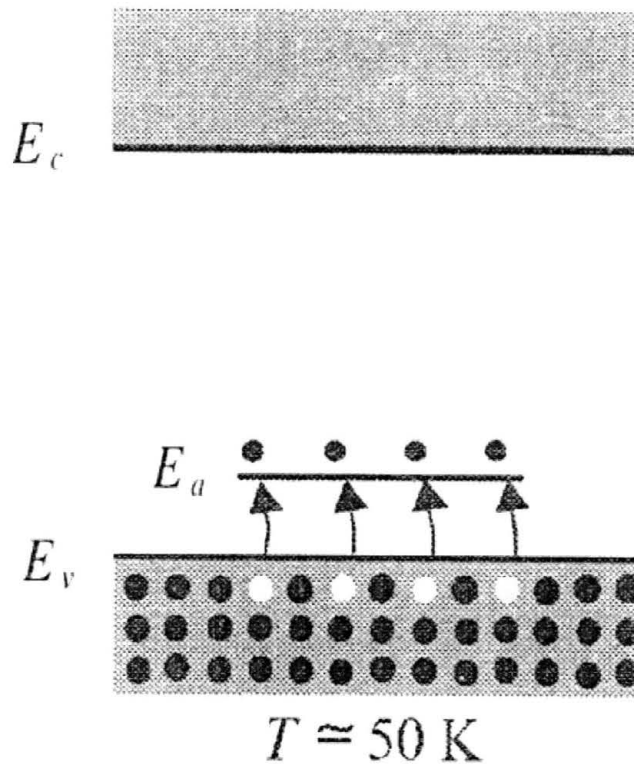


Figure 6: Acceptance of valence band electrons by an acceptor level and creation of holes in the valence band (after Streetman and Banerjee, 2002).

Since this type of impurity level accepts electrons from the valence band, it is called an acceptor level. Impurities from column III of the periodic table are acceptor impurities in silicon (Wilson and Hawkes, 1989; Streetman and Banerjee, 2002).

If silicon is doped with phosphorus an energy level which lies in the range 44 to 45 meV (Person and Bardeen, 1948; Kohn and Luttinger, 1955; Wilson and Hawkes, 1989; Kittel, 1986) below the conduction band is introduced into the energy gap. Infrared absorption experiments at low temperatures have shown that other energy levels exist between the donor level and the conduction band of phosphorus-doped silicon. These give rise to hydrogen-like spectra. The Effective Mass Theory (Ramdas and Rodriguez, 1981) can be used to explain these spectra.

### Effective Mass Theory

In the silicon crystal lattice each silicon atom forms covalent bonds with its four nearest neighbors (Person and Bardeen, 1948). Consider a situation in which silicon is doped with a group V element such as phosphorus. Research using x-rays has shown that phosphorus atoms occupy substitutional positions in the crystal lattice (Person and Bardeen, 1948; Kittel, 1986). The phosphorus atom forms covalent bonds with its four nearest neighbors. Silicon atoms have four valence electrons while phosphorus atoms have five valence electrons. A phosphorus atom contributes one valence electron to each of the four covalent bonds that it forms with its four nearest neighbors. This leaves one valence electron weakly bound to its parent atom (Kittel and Mitchell, 1954; Wilson and Hawkes, 1989; Streetman and Banerjee, 2002). Because of the weak force of attraction between the electron and its parent atom we can consider the electron to be moving in an orbit of several lattice constants (Omar, 1993). The charge on the phosphorus atom is  $+e$ . This situation is similar to that of the hydrogen atom (Person and Bardeen, 1948; Kohn,

1957a; Wilson and Hawkes, 1989) which has a nucleus of charge  $+e$  with a single electron moving around it. The energy levels in the hydrogen atom are given by

$$E_n = -\frac{me^4}{2(4\pi\epsilon_0)^2 n^2 \hbar^2} \quad (1)$$

where  $n = 1, 2, 3, \dots$  and

$$a_0 = \frac{4\pi\epsilon_0 \hbar^2}{me^2} \quad (2)$$

is the Bohr radius. The Bohr theory of the hydrogen atom needs to be modified when it is applied to the situation under consideration. These adjustments are necessary because the electron in this case moves in a solid rather than in a vacuum (Wilson and Hawkes, 1989). Since the electron is moving in the crystal lattice of silicon, the conductivity effective mass  $m^*$  of an electron in silicon should be used instead of the mass of a free electron (Kohn, 1957a; Kittel, 1986). The relative permittivity of the semiconductor must also be included in the derivation of the energy levels. This is because the electron orbit is large enough to embrace a significant number of silicon atoms so that the electron can be considered to be moving in a dielectric medium of relative permittivity  $\epsilon_r$  (Kohn, 1957b; Kittel, 1986; Wilson and Hawkes, 1989; Omar, 1993). Taking these two factors into account, the energy levels will then be given by

$$E_n = -\frac{m^* e^4}{2(4\pi\epsilon_0 \epsilon_r)^2 n^2 \hbar^2} \quad (3)$$

In this case the Bohr radius is given by

$$a^* = \frac{4\pi\epsilon_r\epsilon_0\hbar^2}{m^*e^2} \quad (4)$$

For silicon  $\epsilon_r$  is 11.8 and the conductivity effective mass is 0.26m where m is the rest mass of an electron. This gives  $a^* = 45.4a_0 = 24.1 \text{ \AA}$ . This clearly shows that the radius of orbit of the donor electron is far larger than that of a silicon atom (1.11  $\text{\AA}$ ).

The hydrogenic model of donors suggests observation of spectra similar to the well-known Lyman, Balmer, etc. series of the hydrogen atom (Ramdas and Rodriguez, 1981; Mayur *et al.*, 1993). Given that the donor ionization energy of phosphorus in silicon is around 45 meV, the spectra can be expected in the near to far infrared. The low ionization energy also implies that samples will have to be held at cryogenic temperatures in order to have neutral donors (Ramdas and Rodriguez, 1981). These spectra have been observed. Figure 7 shows a typical excitation spectrum of phosphorus donors in silicon doped with phosphorus. The measurements were taken with the sample at liquid helium temperature. A series of sharp lines is obtained in the range 32-45 meV (Ramdas and Rodriguez, 1981). Other workers (Mayur *et al.*, 1993; Grunt *et al.*, 1997; Donnelly *et al.*, 1997; Lynch *et al.*, 2010) obtained the same results under similar conditions. The spectra are due to electric dipole transitions from the 1s ground state to the excited p states, that is, they are Lyman transitions  $1s \rightarrow np$ ,  $n = 2, 3, 4, \dots$ ”The labeling of the lines denotes the final state of the transition involved and assignment is based on a comparison of the experimentally observed spacings with those deduced from the binding energies of the p states calculated by Faulker (1969) ...” (Ramdas and Rodriguez, 1981).

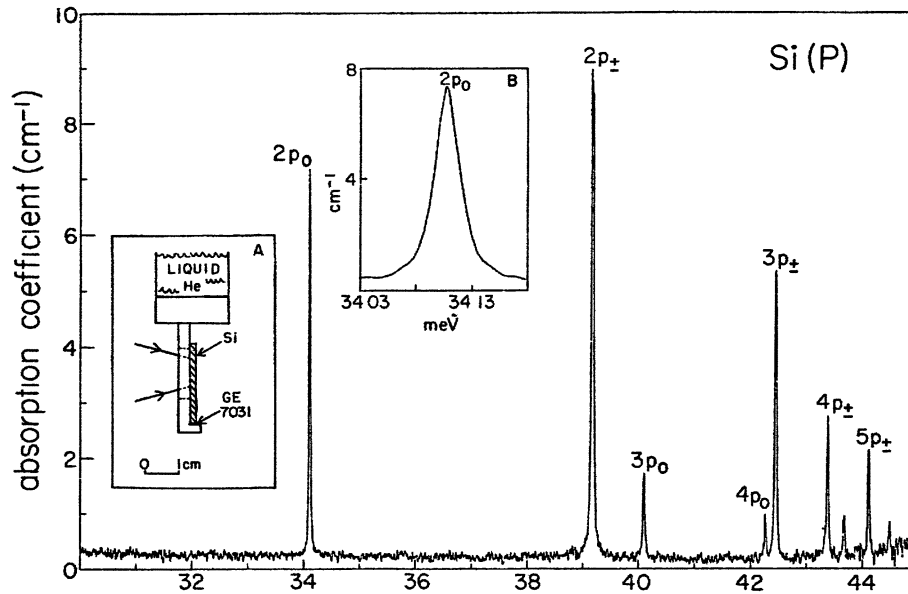


Figure 7: Excitation spectrum of phosphorus donors in silicon doped with phosphorus at liquid helium temperature (after Jagannath *et al.* 1981).

The calculated binding energies are given in table 1. The table shows that there is excellent agreement between the theoretical and experimental values except for the binding energies of the 1s energy levels where there are large discrepancies between theory and experiment. Kohn and Luttinger (1955) also obtained similar results.

There is a general consensus that the effective mass theory gives excellent results for large orbits but fails in regions close to the donor nucleus (Kohn and Luttinger, 1955; Kohn, 1957b; Ramdas and Rodriguez, 1981). The failure in the immediate vicinity of the donor nucleus is attributed to the splitting of the 1s level.

Table 1: Binding energies of some energy levels of substitutional phosphorus in silicon (meV).

Level	Energy (meV)	Theory	Position (cm <sup>-1</sup> )
1s(A <sub>1</sub> )	45.59	31.27	
1s(T <sub>2</sub> )	33.89	31.27	
2p <sub>0</sub>	11.48	11.51	275.09
2p <sub>±</sub>	6.40	6.40	315.95
3p <sub>0</sub>	5.47	5.48	323.42
3d <sub>0</sub>	3.73	3.75	336.8; 337.6
4p <sub>0</sub>	3.31	3.33	340.84
3p <sub>±</sub>	3.12	3.12	342.42

However, this splitting turns out to be significant only for the ground state (Ramdas and Rodriguez, 1981). According to group theory, donor states in group V donors in Silicon have a sixfold degeneracy which arises from the six conduction band minima (Ramdas and Rodriguez, 1981; Mayur *et al.*, 1993) in silicon. For silicon, the departure from a

spherically symmetric Coulomb potential in the immediate vicinity of the donor site lifts the sixfold degeneracy of the  $1s(A_1 + E + T_2)$  ground state and resolves it into a singlet  $1s(A_1)$ , a doublet  $1s(E)$  and a triplet  $1s(T_2)$  (Ramdas and Rodriguez, 1981; Mayur *et al.*, 1993). This splitting is referred to as valley-orbit or chemical splitting. Theoretical considerations suggest that the  $1s(E)$  and the  $1s(T_2)$  levels have binding energies close to those calculated for the  $1s$  level in the effective mass approximation (Long and Myers, 1959; Ramdas and Rodriguez, 1981). Figure 8 shows the energy level scheme based on these considerations. The  $1s(A_1)$  level is significantly shifted below the theoretical value as shown in figure 8. This shift explains the large discrepancy of about 14.32 meV between the theoretical value of the donor ionization energy obtained using the effective mass theory and the experimental value (Long and Myers, 1959). At liquid helium temperatures only the  $1s(A_1)$  level is occupied by the donor electron and hence one measures the  $1s(A_1) \rightarrow np_o$ ,  $1s(A_1) \rightarrow np_{\pm}$  series (Ramdas and Rodriguez, 1981; Mayur *et al.*, 1993) where  $n = 1, 2, 3, \dots$ . If the sample is held at appropriate temperatures between liquid helium temperature and liquid nitrogen temperature, the  $1s(E)$  and the  $1s(T_2)$  levels get thermally populated (Lynch *et al.*, 2010). In this case the excitation spectra that will be observed correspond to the  $1s(E) \rightarrow np_o$ ,  $1s(E) \rightarrow np_{\pm}$  and  $1s(T_2) \rightarrow np_o$ ,  $1s(T_2) \rightarrow np_{\pm}$  transitions (Ramdas and Rodriguez, 1981; Mayur *et al.*, 1993).

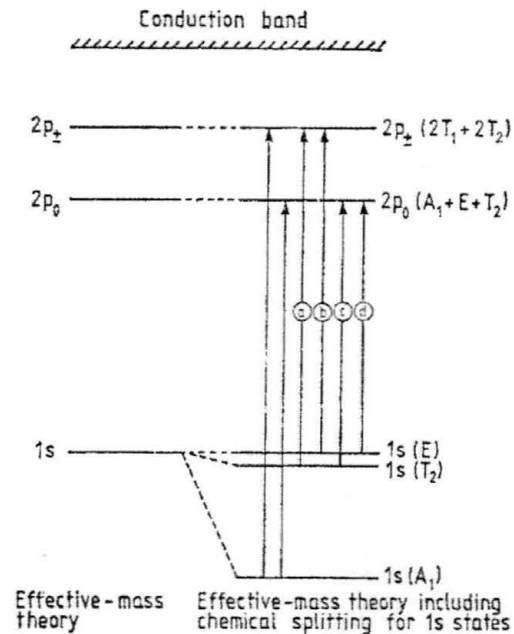


Figure 8: Energy level scheme of group V impurities in silicon for transitions from the 1s states to the  $2p_0$ ,  $2p_{\pm}$  states (after Ramdas and Rogriguez 1981).

The presence of impurities which are acceptors (for example boron) in silicon samples doped with phosphorus can result in additional lines in the wave number range in which the above spectra are expected. The next section gives details on how the spectra due to the acceptors arise.

### Spectra due to Acceptors

The electron states at the valence band edge of silicon and other semiconductors are p-like (orbital quantum number  $l = 1$ ) (Winkler, 2003). Due to spin-orbit interaction, the total angular momentum  $j$  of these states is given by  $j = l \pm s$  where  $l$  is the orbital angular momentum and  $s$  is the spin angular momentum (Mahan, 2009). Since  $l = 1$

and  $s = \pm \frac{1}{2}$ , the total angular momentum will be  $j = \frac{3}{2}$  or  $j = \frac{1}{2}$  (Ramdas and Rodriguez, 1981; Winkler, 2003). The states associated with  $j = \frac{3}{2}$  and  $j = \frac{1}{2}$  are split in energy by a gap  $\lambda$  (Pankove, 1975; Ramdas and Rodriguez, 1981). Since this splitting is due to spin-orbit interaction it is referred to as spin-orbit splitting. States associated with  $j = \frac{3}{2}$  are denoted  $p_{3/2}$  while those associated with  $j = \frac{1}{2}$  are denoted  $p_{1/2}$ . This gives the  $p_{3/2}$  and the  $p_{1/2}$  valence subbands. Figure 9 shows the detailed structure of the valence band of silicon together with the associated acceptor states. The arrows show the transitions from the ground state in the band gap ( $I_g$ ) to the excited states associated with the  $p_{3/2}$  and the  $p_{1/2}$  valence bands. These transitions are referred to as the  $p_{3/2}$  and the  $p_{1/2}$  series.

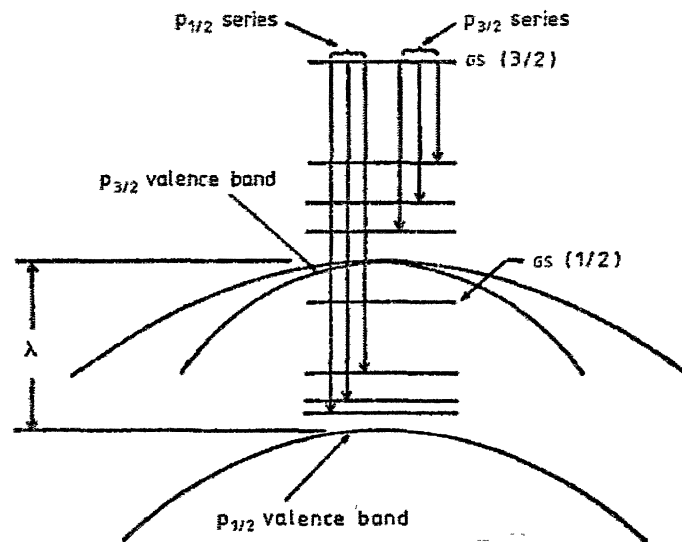


Figure 9: The spin-orbit-split valence band of silicon with associated states. Here GS is the ground state and  $\lambda$  is the spin-orbit splitting at  $k = 0$  (after Ramdas and Rodriguez 1981).

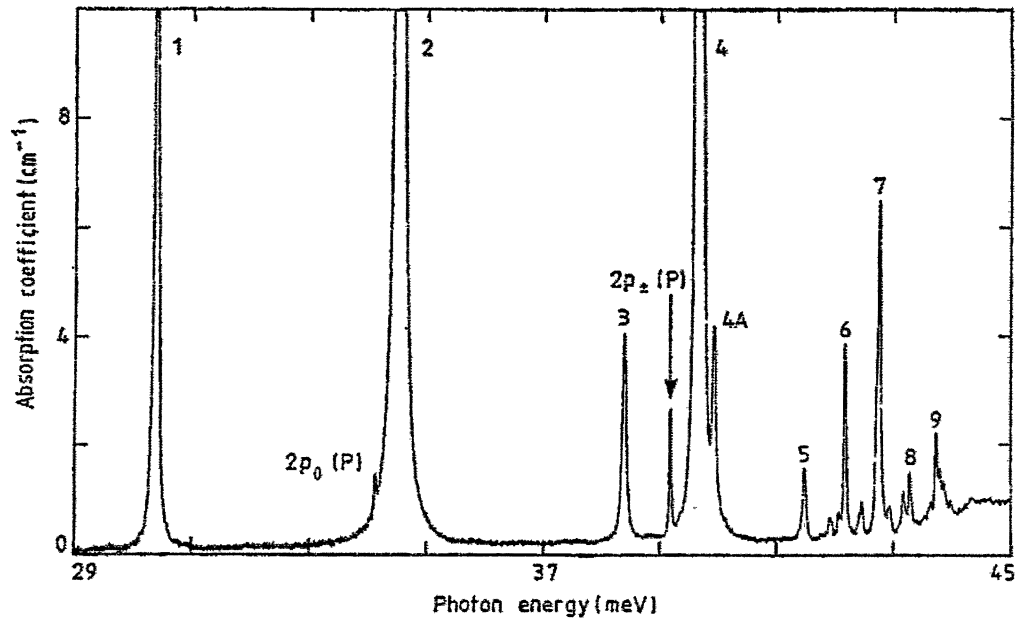


Figure 10: Excitation spectrum of silicon doped with boron. The lines due to phosphorus donors are labeled P in parenthesis. Liquid helium was used as a coolant (after Jagannath *et al.* 1981)

Figure 10 shows the typical excitation spectrum of boron-doped silicon at liquid helium temperatures. These lines belong to the  $p_{3/2}$  series. Table 2 shows frequencies of the boron lines in silicon.

From this discussion it can be concluded that for annealing studies on phosphorus-doped silicon, the mere presence of excitation spectra in the wave number range in which the spectra are expected is not enough to conclude that a particular sample has been annealed as these could be due to the presence of other donors or acceptors in the sample. It is therefore important to ensure that if excitation spectra are observed they occur at the positions given in table 1 before reaching a conclusion as to whether the sample was annealed or not.

Table 2: Position ( $\text{cm}^{-1}$ ) of some of the electronic excitation lines of boron in silicon (after Pajot and Debarre 1981).

1	244.99
2	278.27
3	309.47
4	319.35
4-A	319.96
4-B	321.90
5	334.52; 338.05; 339.41
6	340.13
7	344.75; 346.13
8	348.3; 349.1
9	352.8; 354.1

## CHAPTER III

### METHODS AND MATERIALS

#### Introduction

This chapter gives information on how the samples that were used in the experiments were prepared as well the measurements that were taken in order to determine whether the samples had been annealed after treatment with the laser beam.

#### Sample Preparation

Two silicon wafers each of 4 inches diameter were used in the experiment. The wafers which were supplied by Axcelis Technologies had been grown using the Czochralski technique. Using ion implantation, one of the wafers was doped with phosphorus to a concentration of  $4 \times 10^{14} \text{ cm}^{-3}$  and the other to a concentration of  $1 \times 10^{15} \text{ cm}^{-3}$ . To achieve the doping concentration of  $4 \times 10^{14} \text{ cm}^{-3}$  a dose of  $4 \times 10^{14} \text{ ions cm}^{-2}$  was administered on the wafer using a 40 keV beam of ions. For the  $1 \times 10^{15} \text{ cm}^{-3}$  doping concentration the dose was  $1 \times 10^{15} \text{ cm}^{-2}$  with the energy of the beam ions being the same as that for the other wafer. Ion implantation was done by Coresystems. Each wafer was subjected to four laser pulses, one at each corner of a square of side two inches. The

average energy of the laser pulses was 5 J and the duration of each pulse was 5 ns. The wavelength of the laser beam was 1.06  $\mu\text{m}$ . The power of the laser beam was approximately 1 GW and the diameter about 2 mm. The annealing was done at the Naval Research Laboratories. Each wafer was then broken into pieces each about 1.5 cm by 1.0 cm and three pieces from each wafer were selected at random for analysis.

### Sample Analysis

Two sets of measurements were taken in order to determine whether the doped silicon samples had been annealed or not after subjecting them to laser pulses. These were measurements at room temperature and measurements at liquid helium temperature. In each case, before making measurements, the samples were cleaned using an ultrasonic cleaner. This was done by placing the sample in a beaker of acetone and then immersing the beaker in an ultrasonic cleaner bath for 2 minutes. The procedure was then repeated with isopropyl alcohol. The sample was then dried using a heat gun to ensure that no residue was left on the wafer surface.

### Room Temperature Measurements

These were made using a Nicolet Fourier Transform Infrared (FT-IR) spectrometer, model 6700. The top cover of the sample compartment of the FT-IR was removed and a Janis Supertrans-VP cryostat was lowered into the sample compartment. The sample compartment was then covered with a piece of rubber which had a hole in the middle to

accommodate the cryostat. Masking tape was used to make an airtight seal on the edges of the piece of rubber where it came into contact with the sample compartment. This was done to ensure that nitrogen gas would not leak from the sample compartment through the top. It was important to do this because the sample compartment is supposed to be purged with a gas such as nitrogen which is not infrared active. Allowing air into the sample compartment would result in absorption of the infrared radiation by other gases in the atmosphere such as carbon dioxide and water. This would cause problems in the interpretation of the spectra that are collected.

The cryostat was evacuated for two hours using a Varian Turbo-V 70 pump. After this the background spectrum was then collected using infrared radiation in the range  $200 - 400\text{cm}^{-1}$ . This was done while the pump was still running. An ETC infrared light source provided the infrared radiation and a DTGS TEC detector was used to detect the transmitted beam. An XT-KBr beamsplitter was used. In order to determine if the FT-IR was giving consistent results a sample spectrum was collected without a sample in place. This would yield a 100 % transmission line if the FT-IR was working as expected. The sample spectrum to obtain the 100% transmission line was also collected with the vacuum pump running. The pump was then stopped and the first sample from wafer number 1 was attached to the cold finger of the cryostat using thermal compound. The cryostat was evacuated for a period of 30 minutes after which the sample spectrum of sample 1 was collected. For both the background and sample spectra, 256 scans were averaged. Note that for those room temperature measurements the cryostat's cold finger was not cooled but kept at room temperature. The sample spectrum was collected with the vacuum pump running. This procedure was done for all the six samples from the two

wafers. To check the reproducibility of the results obtained the above procedure was repeated for all the six samples. This was done after the first round of trials had been completed for all the samples.

#### Liquid Helium Temperature Measurements

For each sample the background spectrum and 100% line were collected using the same procedure as that for room temperature measurements except that in this case the vacuum pump was allowed to run for 8 hours or more prior to collecting the background spectrum. A sample was then attached to the cold finger of the cryostat using thermal compound. The cryostat was then evacuated for 30 minutes after which the sample was cooled with liquid helium until the temperature reached about 5K. The temperature was monitored for a few minutes to ensure that it was stable. This temperature was noted and the sample spectrum was then collected. This procedure was done for all the six samples from the two wafers. To check the reproducibility of the results obtained the above procedure was repeated for all the six samples.

## CHAPTER IV

### RESULTS AND DISCUSSION

#### Introduction

In this chapter the results that were obtained in the experiments that were conducted are presented and analyzed.

#### Room Temperature Measurements

Figures 11 to 22 show the spectra that were obtained at room temperature. For each sample, the spectra for the first and second trial look the same. These spectra show a common pattern. In this wavelength range the absorbance decreases with increase in wavelength. Shen and Cardona (1981) obtained similar spectra for lightly doped silicon. The spectra are mainly due to intrinsic absorption of the Si-Si network (Shen and Cardona, 1981). The spectra are greatly influenced by the presence of phosphorus on substitutional lattice sites. The phosphorus impurities add an ionic component to the Si-P bond resulting in increased absorption (Shen and Cardona, 1981). There is noise in all the spectra that were collected. An exhaustive literature search did not shed some light on the likely source of the noise.

Tables 3 and 4 show the positions of the peaks ( $\text{cm}^{-1}$ ) for the spectra that were collected for the various samples at room temperature. For Sample 2 of wafer 1 and all the samples for wafer 2 the peaks are found at the same positions. Sample 2 of wafer 1 and sample 3 of wafer 2 have two additional peaks located at  $272.2 \text{ cm}^{-1}$  and  $322.7 \text{ cm}^{-1}$ . The peaks for samples 1 and 3 of wafer 1 occur at frequencies which are different from those of the other four samples. These two samples though have common peaks at  $229.6 \text{ cm}^{-1}$  and around  $276.5 \text{ cm}^{-1}$ . We are not able to identify the phenomena responsible for producing these peaks.

Table 3: Observed peaks ( $\text{cm}^{-1}$ ) for samples from wafer 1. Measurements were done at room temperature.

Sample 1		Sample 2		Sample 3	
Trial 1	Trial 2	Trial 1	Trial 2	Trial 1	Trial 2
205.4	205.4	222.0	222.0	229.6	229.6
229.5	229.5	255.5	255.5	249.2	249.4
276.4	276.5	272.2	272.2	276.9	277.2
304.1	304.1	283.8	283.8	288.4	288.4
329.3	329.3	297.1	297.1	316.2	316.2
348.3	348.4	322.7	322.8	343.9	344
		353.3	353.0		

Table 4: Observed peaks ( $\text{cm}^{-1}$ ) for samples from wafer 2. Measurements were done at room temperature.

Sample 1		Sample 2		Sample 3	
Trial 1	Trial 2	Trial 1	Trial 2	Trial 1	Trial 2
222.0	222.0	222.0	222.0	222.0	222.0
255.6	255.5	255.7	255.7	255.3	255.4
283.9	283.8	284	284	272.2	272.2
297.5	297.3	297.6	297.6	283.6	283.6
350.9	350.9	350.9	350.9	296.9	297
				322.2	322.4
				353	353.2

### Liquid Helium Temperature Measurements

Figures 23 to 34 show the spectra that were obtained at liquid helium temperatures. The temperatures of the samples were steady at 5 K as the spectra were collected. A sample which has been annealed is expected to exhibit the characteristic lines as indicated in table 1. In particular, for phosphorus, the  $2 p_{\pm}$  line is expected to be the most intense line (Parot and Debarre, 1981). Tables 5 and 6 show the positions of the electronic excitation lines which were observed for samples from the two wafers which were analyzed. Only lines in the frequency range  $275 \text{ cm}^{-1}$  to  $350 \text{ cm}^{-1}$  were considered since this is where we expect to find phosphorus excitation lines in silicon for samples held at liquid helium temperatures. A comparison of table 1 and tables 5 and 6 shows that none of the characteristic lines is present in the spectra that were collected. We can therefore

conclude that the samples were not annealed. The results obtained thus seem to suggest that some parts of the wafer were not annealed. It would seem reasonable to increase the number of points at which the laser pulses are applied in order to anneal the whole wafer.

The lines that are marked on the spectra appear to be boron lines. Table 2 in chapter 2 shows the frequencies at which boron lines are expected. Boron is a contaminant present in silicon wafers which are grown using the Czochralski technique. The boron spectral lines 4-4A and 2 are the most intense and are of about equal intensities in line with the findings by Parot and Debarre (1981). These characteristic boron lines are absent from the spectra for the first trials of samples 1 and 2 from wafer 2. However, these lines are present in the second trials. It can be speculated that the absence of the boron lines from the first trials is probably due to the fact that sample temperatures were not low enough.

Table 5: Observed electronic excitation lines ( $\text{cm}^{-1}$ ) for samples from wafer 1.

Sample 1		Sample 2		Sample 3	
Trial 1	Trial 2	Trial 1	Trial 2	Trial 1	Trial 2
278.7	278.6	277.9	277.7	276.9	276.8
318.2	318.5	320.3	320.1	319.2	319.2
320.3	320.1			321	321.1
348.5	329.6				
	346.1				

Table 6: Observed electronic excitation lines ( $\text{cm}^{-1}$ ) for samples from wafer 2.

Sample 1		Sample 2		Sample 3	
Trial 1	Trial 2	Trial 1	Trial 2	Trial 1	Trial 2
277.7	277.7	334.4	277.5	280.6	277.5
320.1	320.1	283.6	280.6	282.5	320.3
			297.0	333.5	
			309.8	336.6	
			319.8		
			348.3		

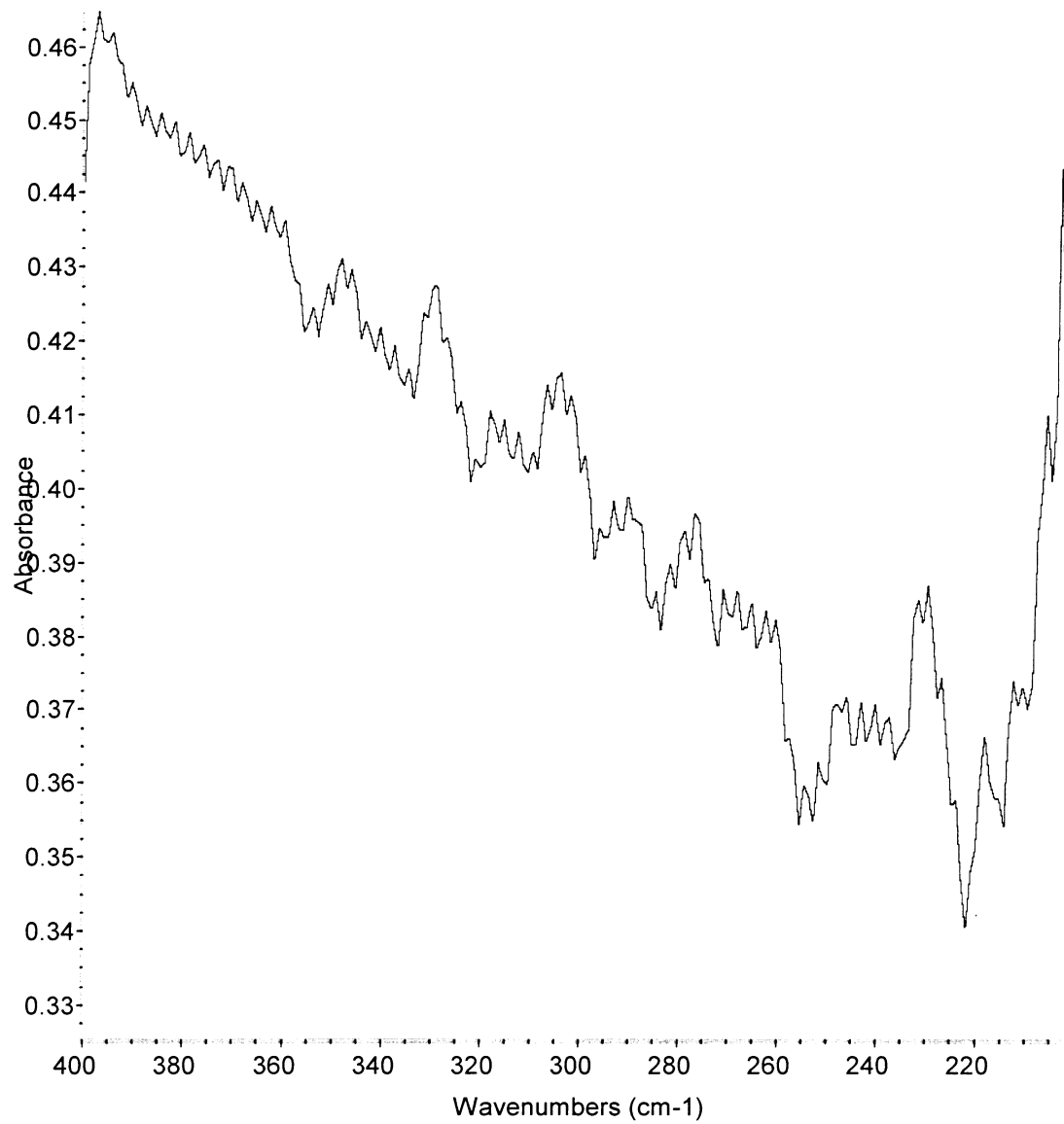


Figure 11: Spectrum for sample 1 of wafer 1, trial 1. Measurements were done at room temperature.

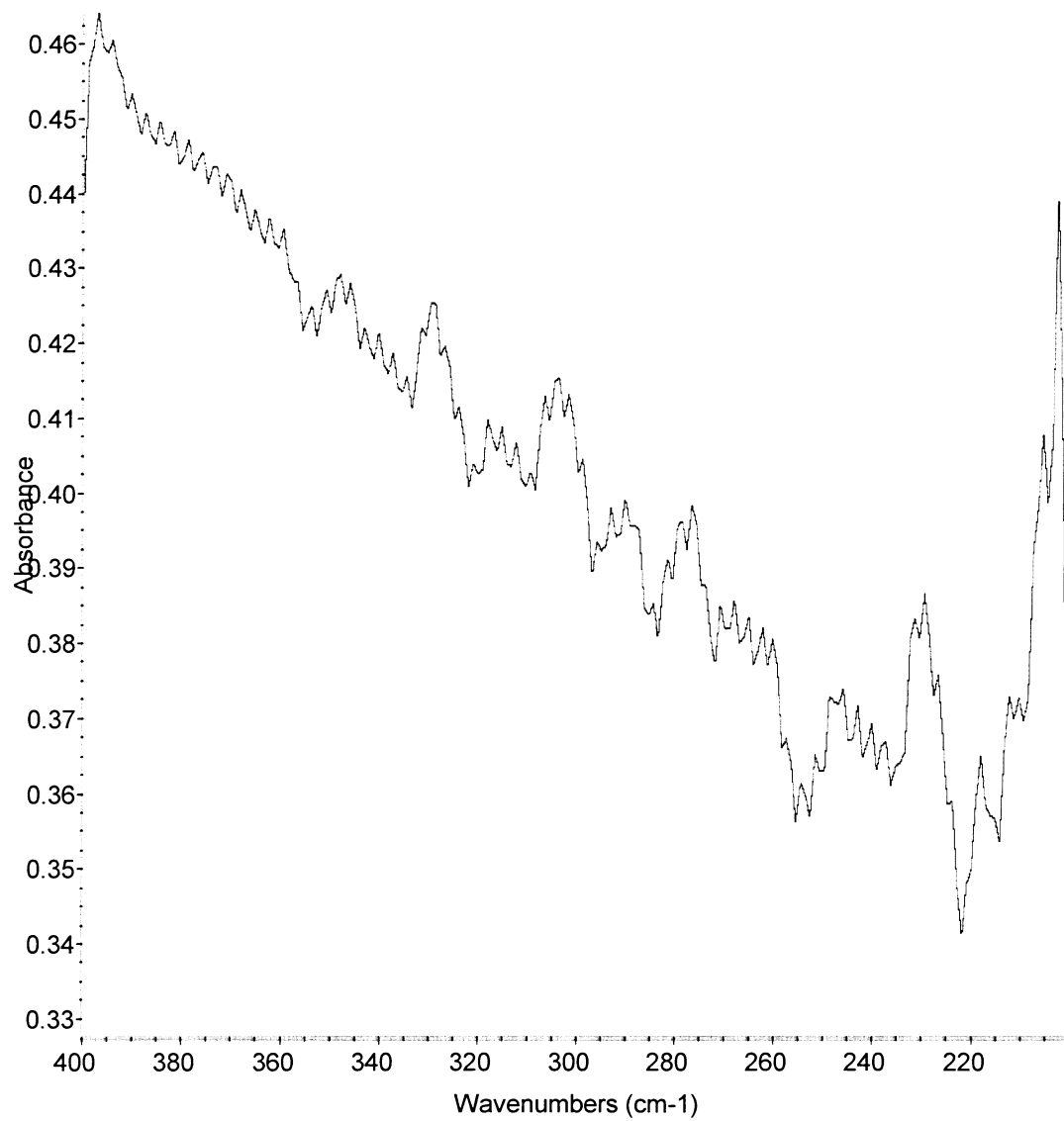


Figure 12: Spectrum for sample 1 of wafer 1, trial 2. Measurements were done at room temperature.

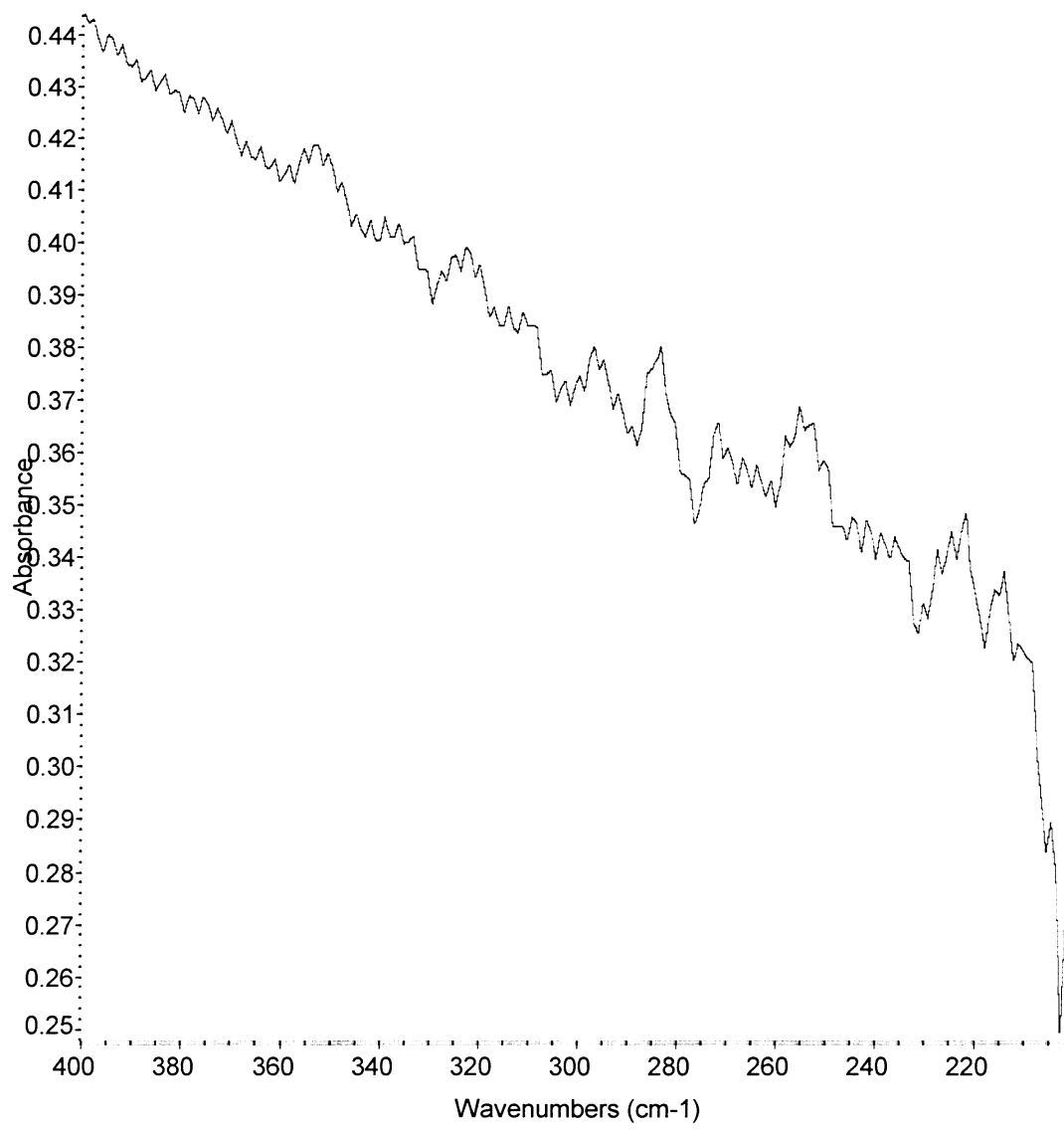


Figure 13: Spectrum for sample 2 of wafer 1, trial 1. Measurements were done at room temperature.

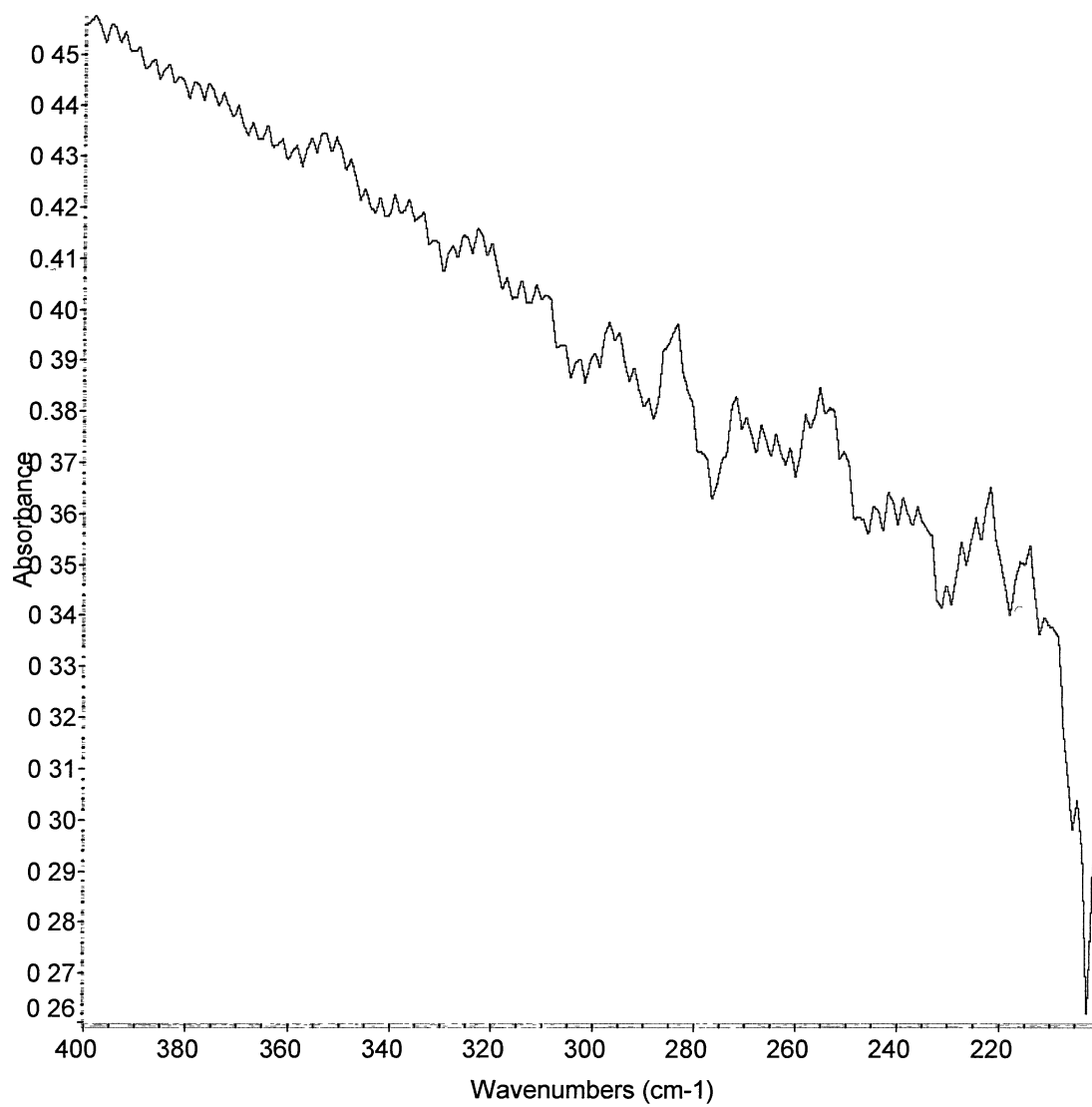


Figure 14: Spectrum for sample 2 of wafer 1, trial 2. Measurements were done at room temperature.

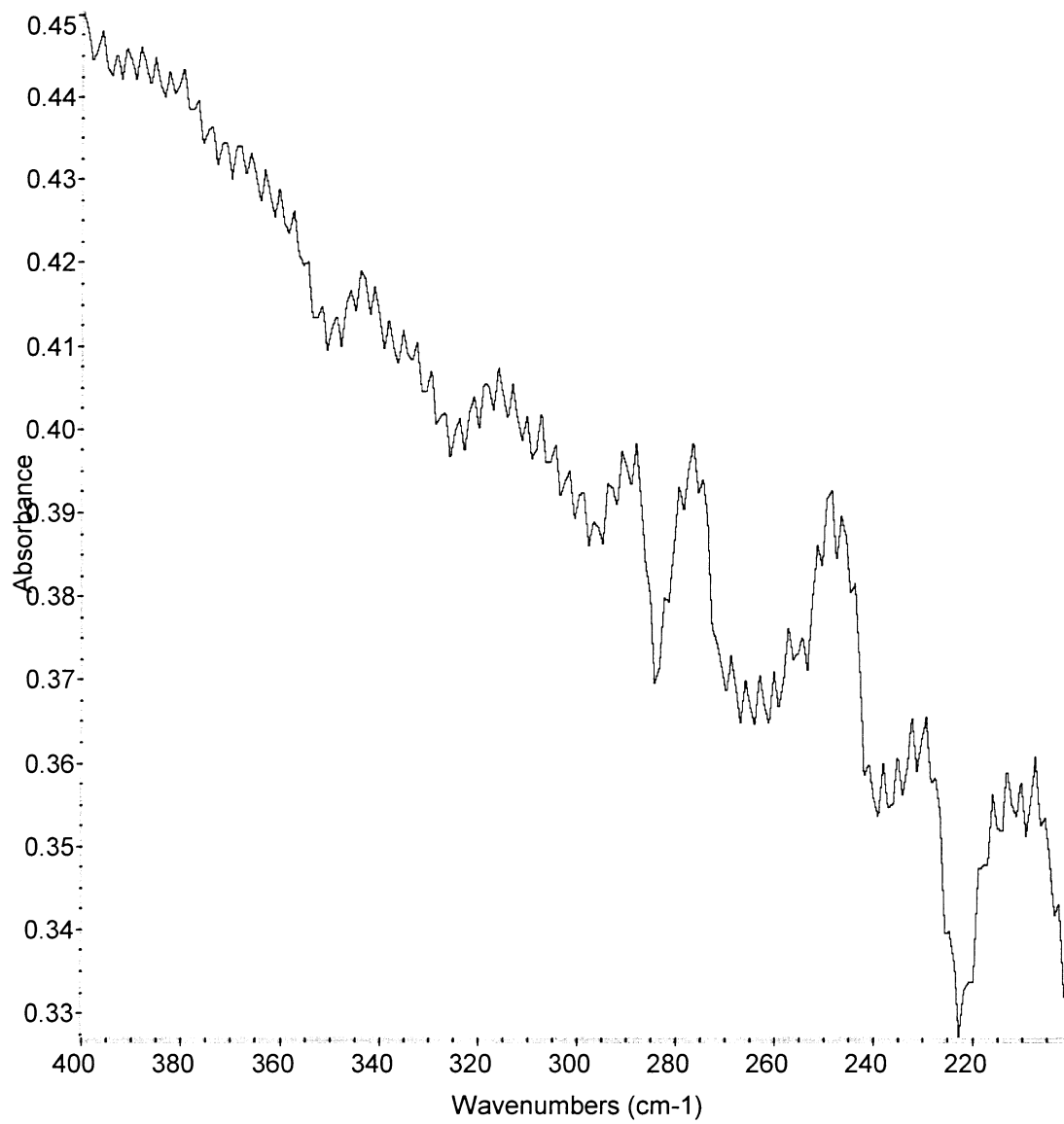


Figure 15: Spectrum for sample 3 of wafer 1, trial 1. Measurements were done at room temperature.

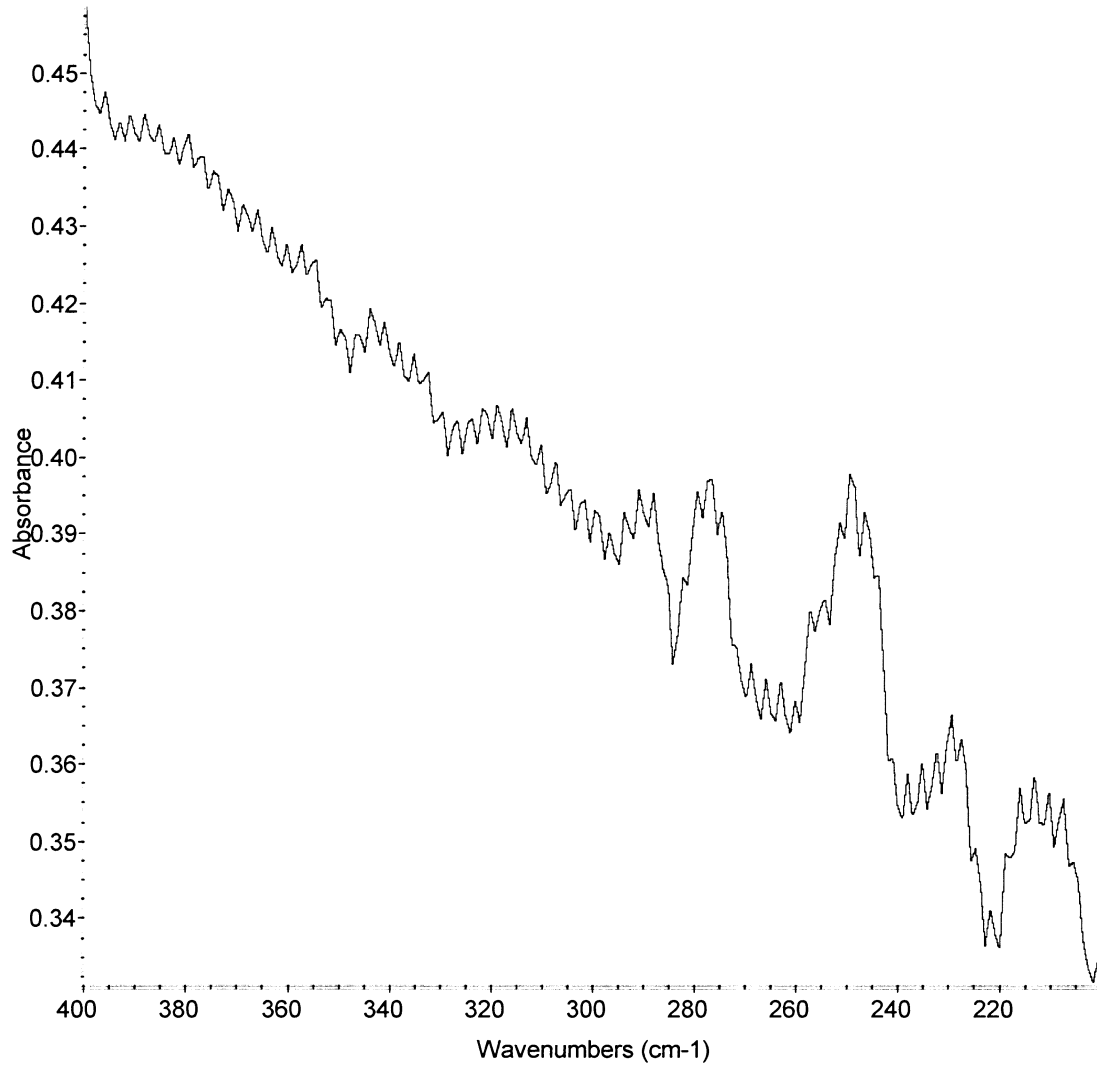


Figure 16: Spectrum for sample 3 of wafer 1, trial 2. Measurements were done at room temperature.

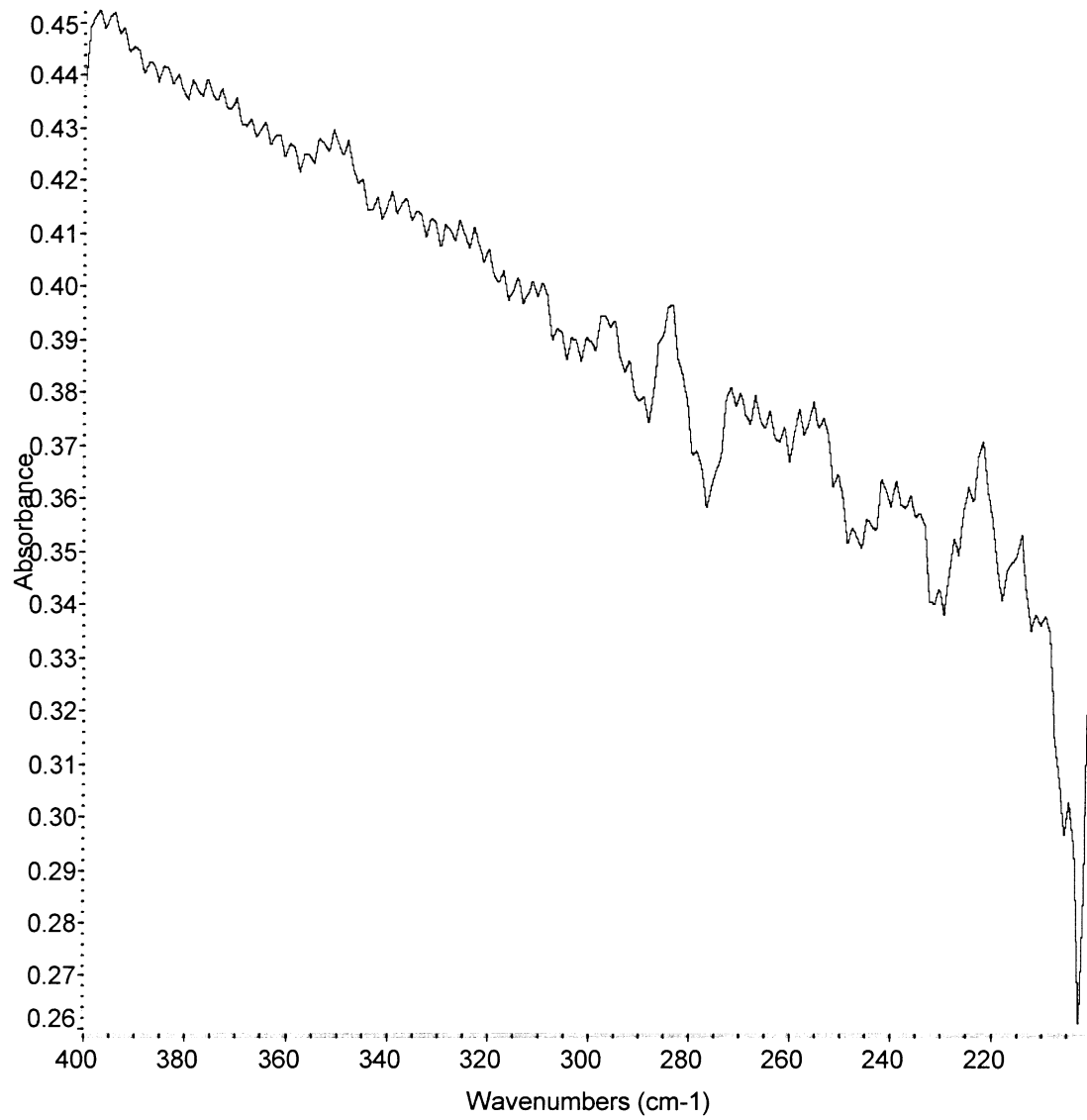


Figure 17: Spectrum for sample 1 of wafer 2, trial 1. Measurements were done at room temperature.

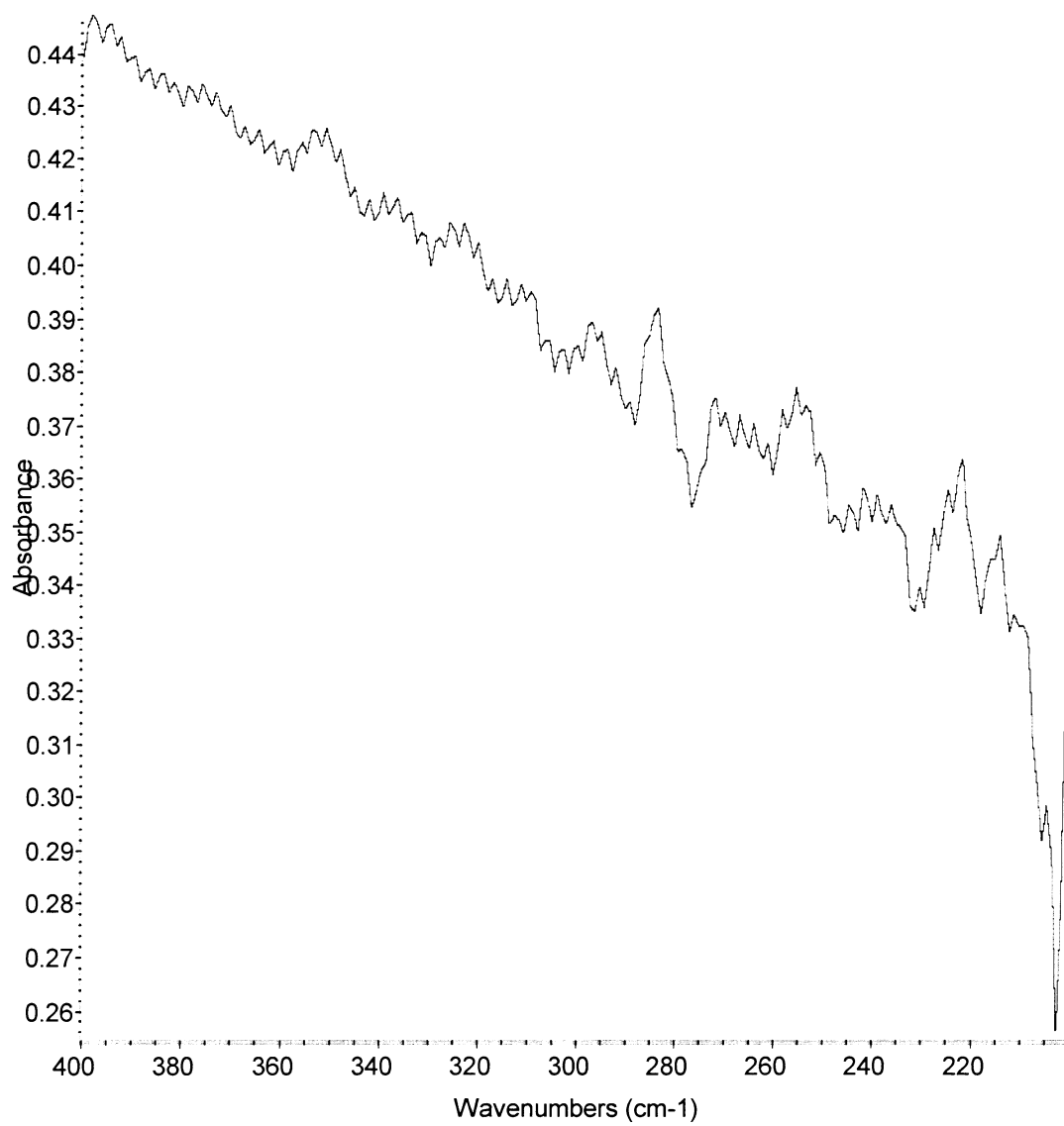


Figure 18: Spectrum for sample 1 of wafer 2, trial 2. Measurements were done at room temperature.

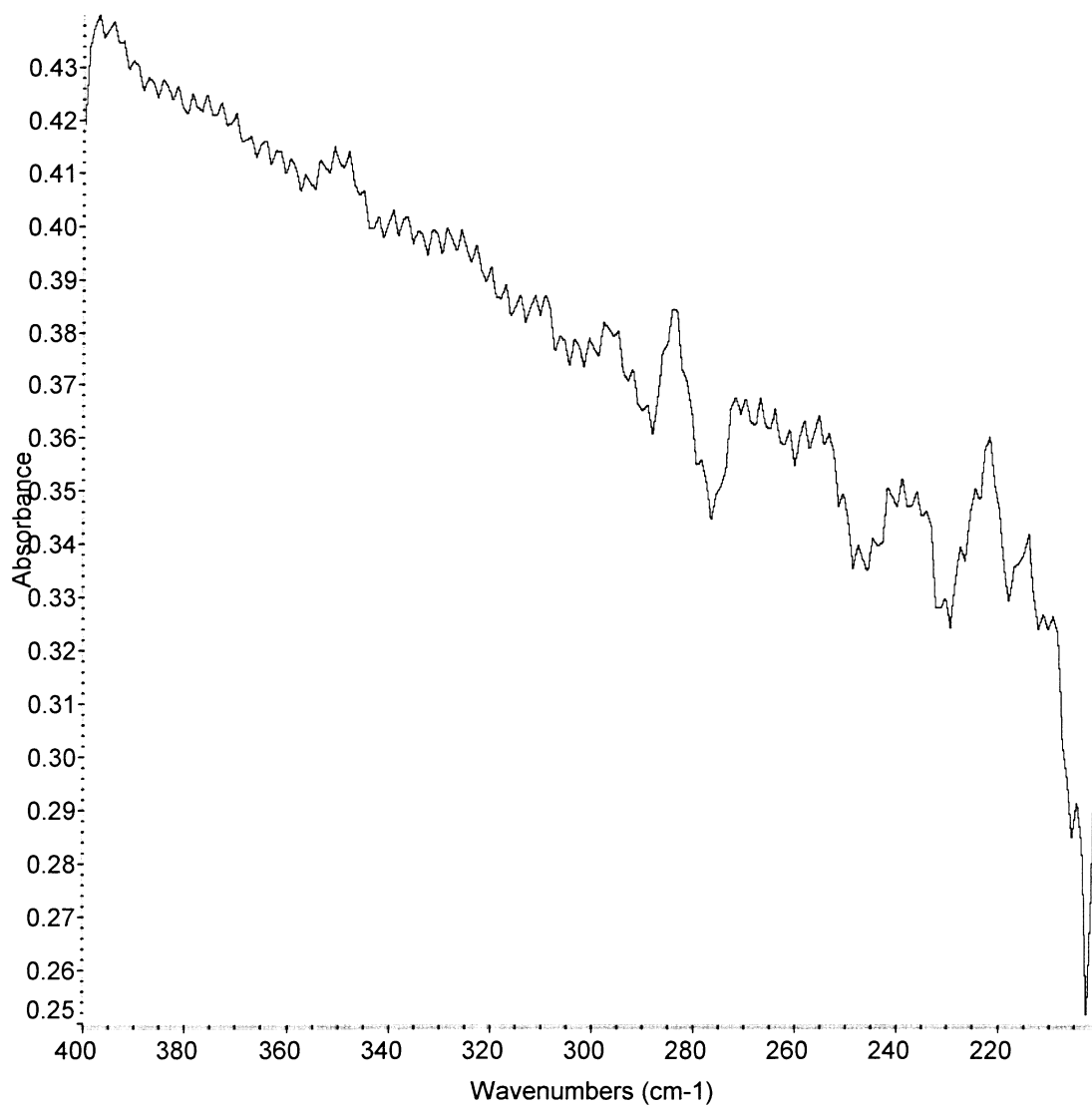


Figure 19: Spectrum for sample 2 of wafer 2, trial 1. Measurements were done at room temperature.

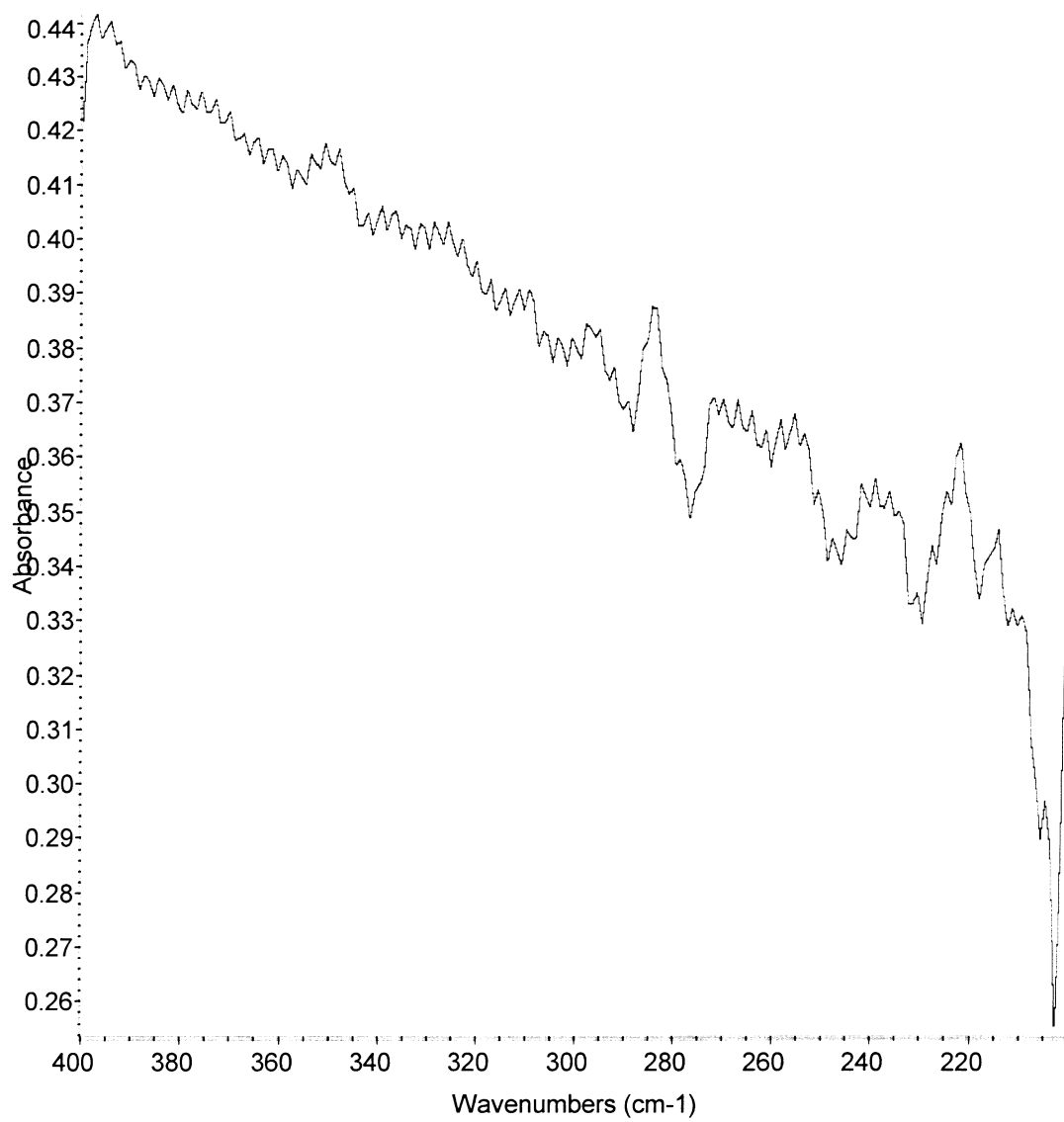


Figure 20: Spectrum for sample 2 of wafer 2, trial 2. Measurements were done at room temperature.

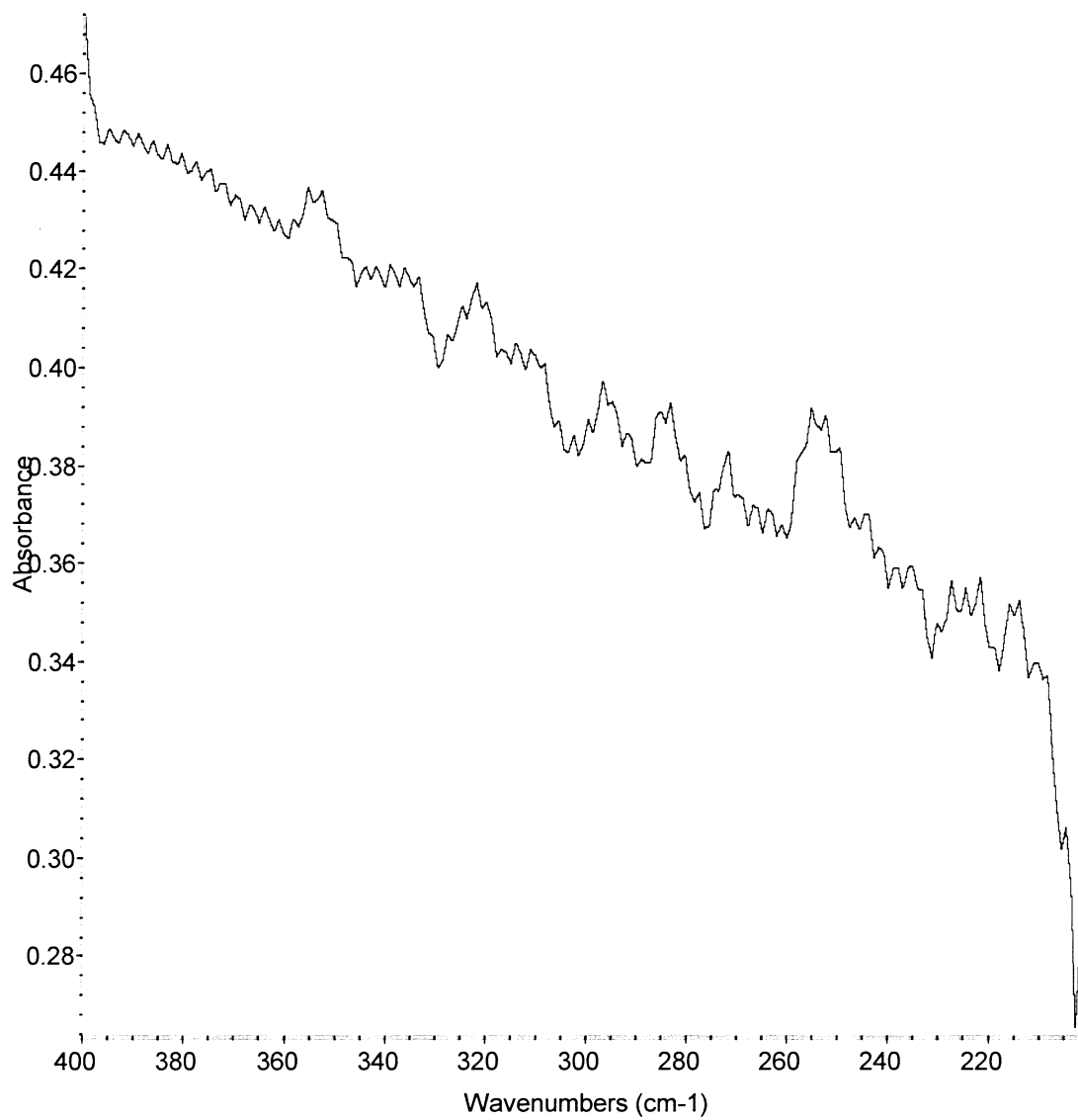


Figure 21: Spectrum for sample 3 of wafer 2, trial 1. Measurements were done at room temperature.



Figure 22: Spectrum for sample 3 of wafer 2, trial 2. Measurements were done at room temperature.

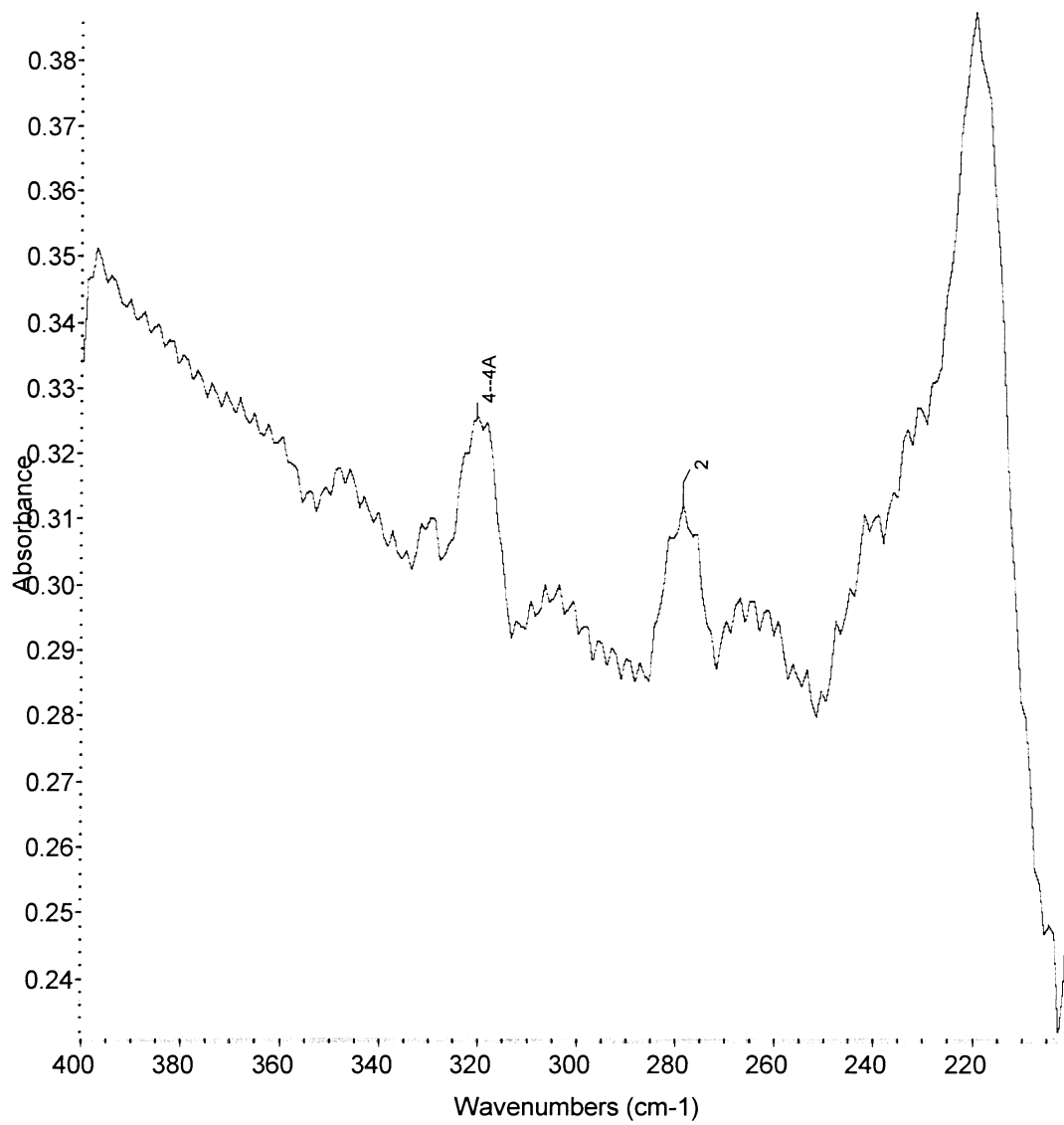


Figure 23: Spectrum for sample 1 of wafer 1, trial 1. Measurements were done at liquid helium temperature. The lines marked are boron excitation lines.

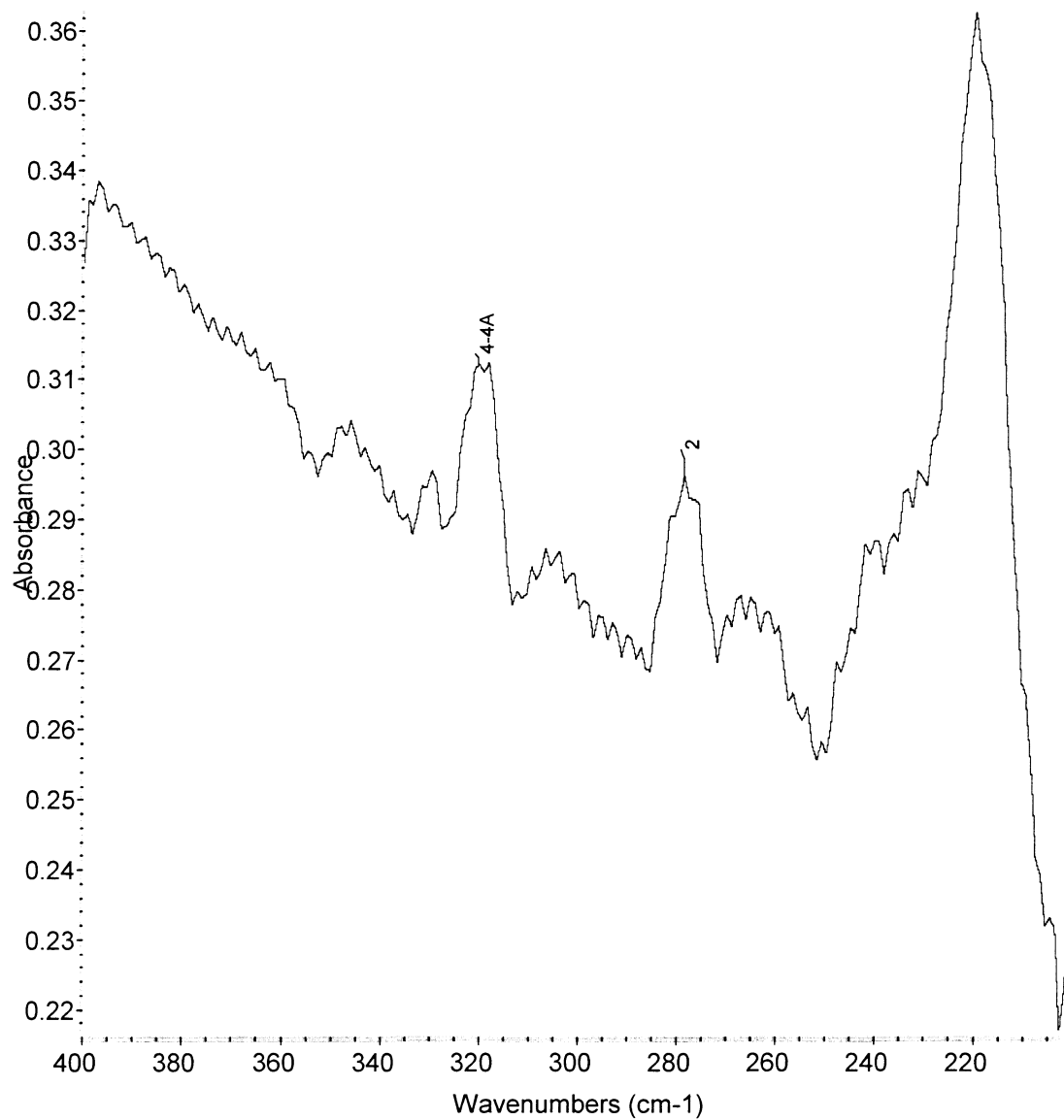


Figure 24: Spectrum for sample 1 of wafer 1, trial 2. Measurements were done at liquid helium temperature. The lines marked are boron excitation lines.

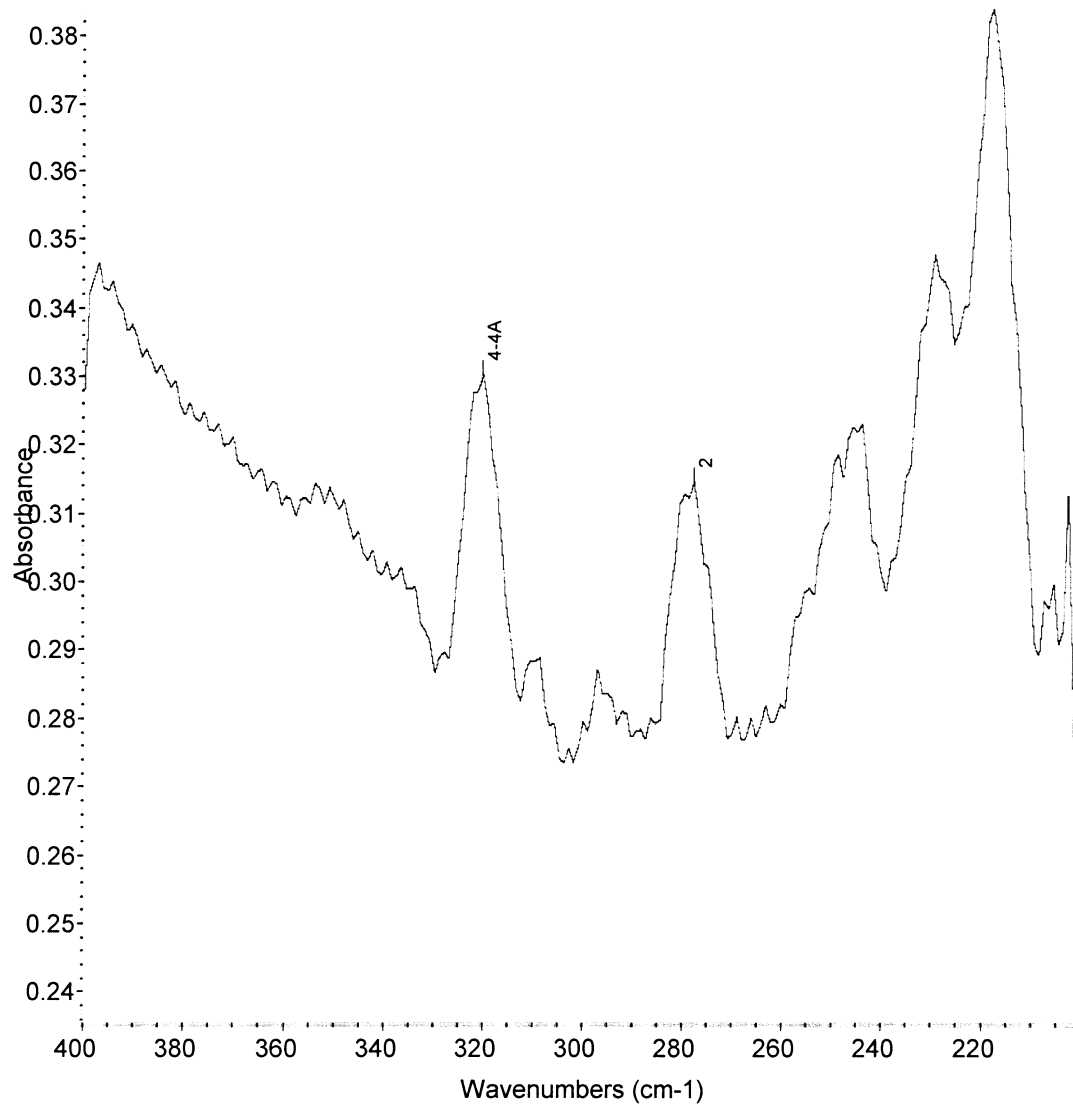


Figure 25: Spectrum for sample 2 of wafer 1, trial 1. Measurements were done at liquid helium temperature. The lines marked are boron excitation lines.

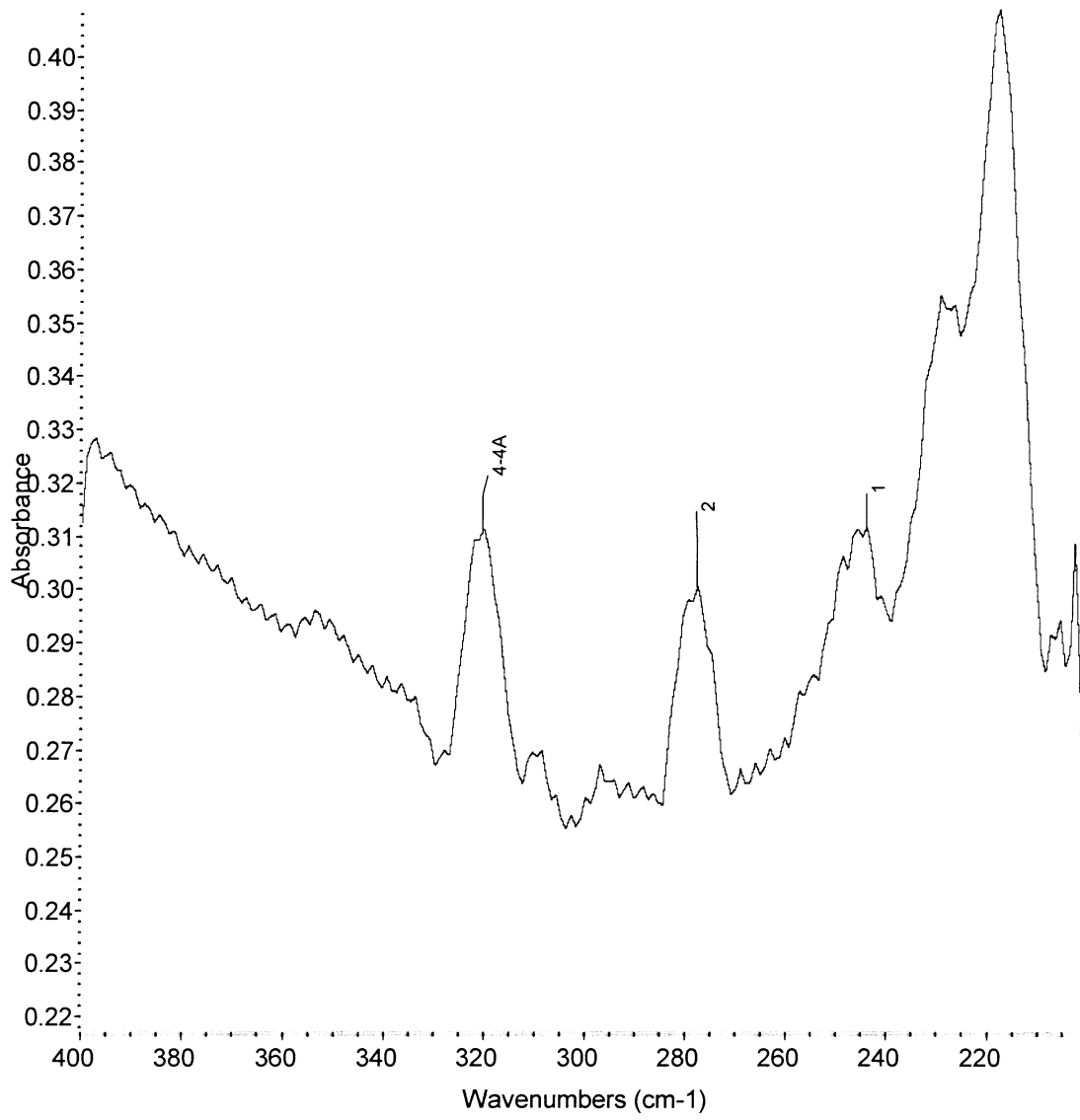


Figure 26: Spectrum for sample 2 of wafer 1, trial 2. Measurements were done at liquid helium temperature. The lines marked are boron excitation lines.

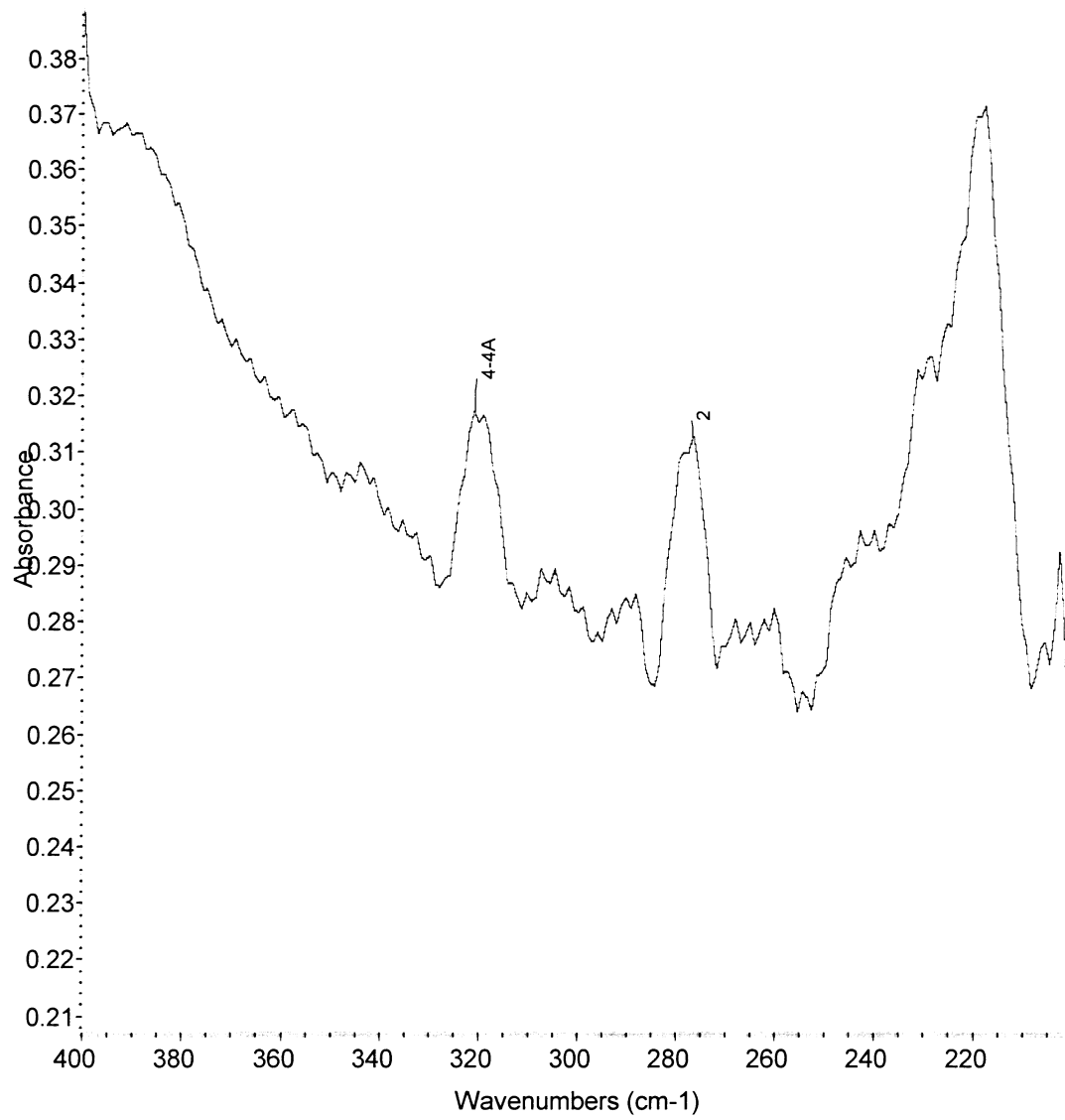


Figure 27: Spectrum for sample 3 of wafer 1, trial 1. Measurements were done at liquid helium temperature. The lines marked are boron excitation lines.

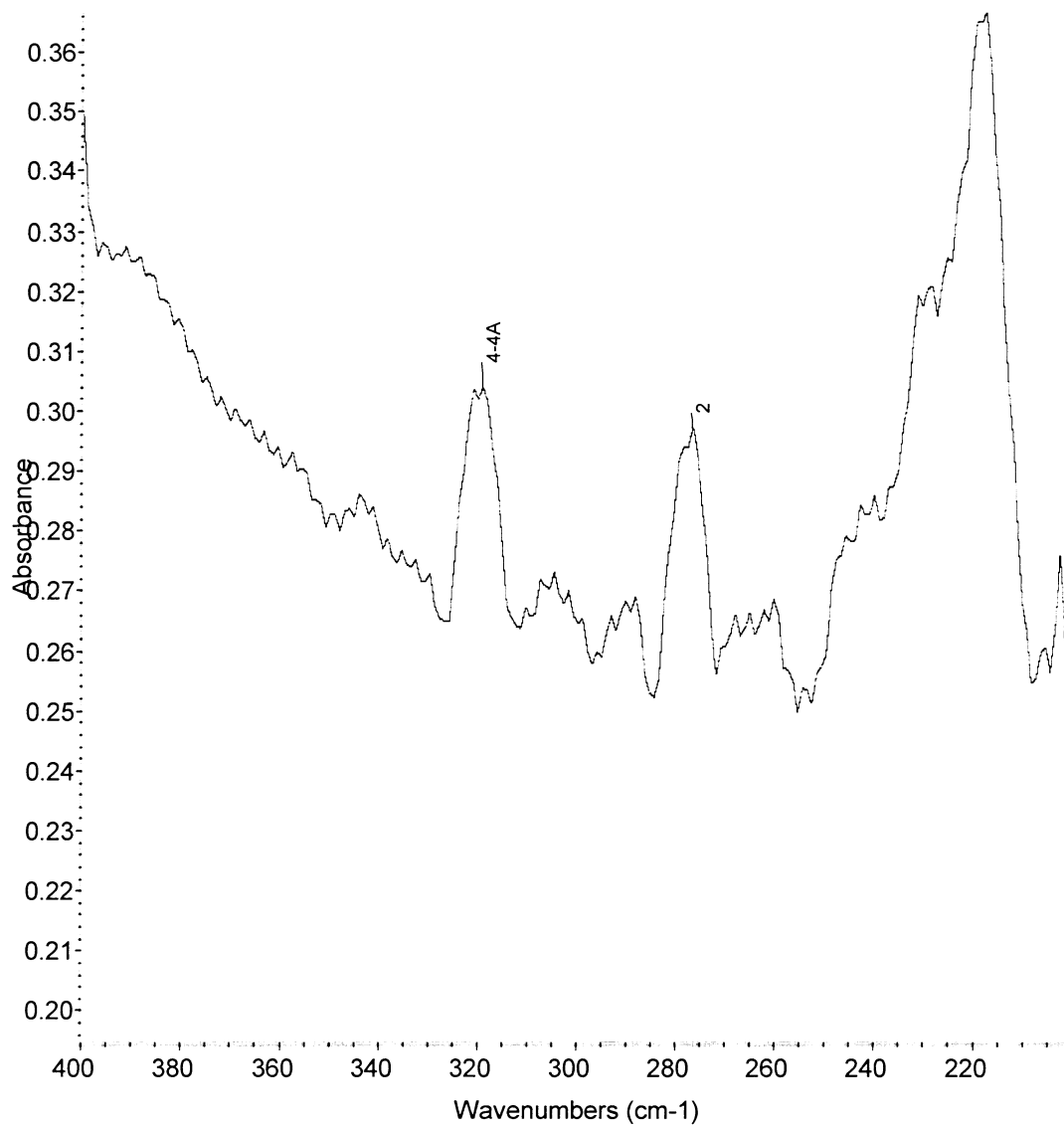


Figure 28: Spectrum for sample 3 of wafer 1, trial 2. Measurements were done at liquid helium temperature. The lines marked are boron excitation lines.

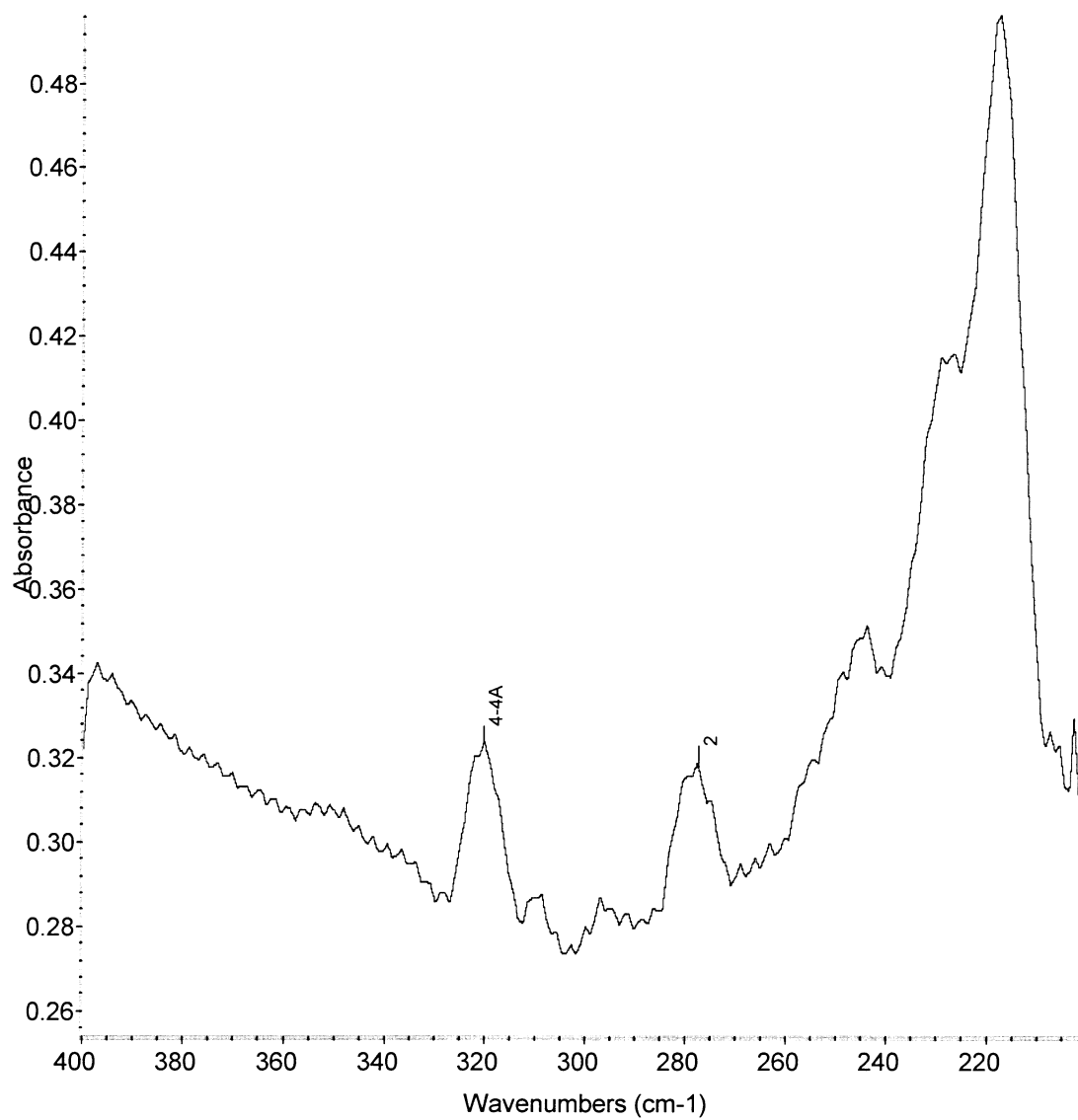


Figure 29: Spectrum for sample 1 of wafer 2, trial 1. Measurements were done at liquid helium temperature. The lines marked are boron excitation lines.

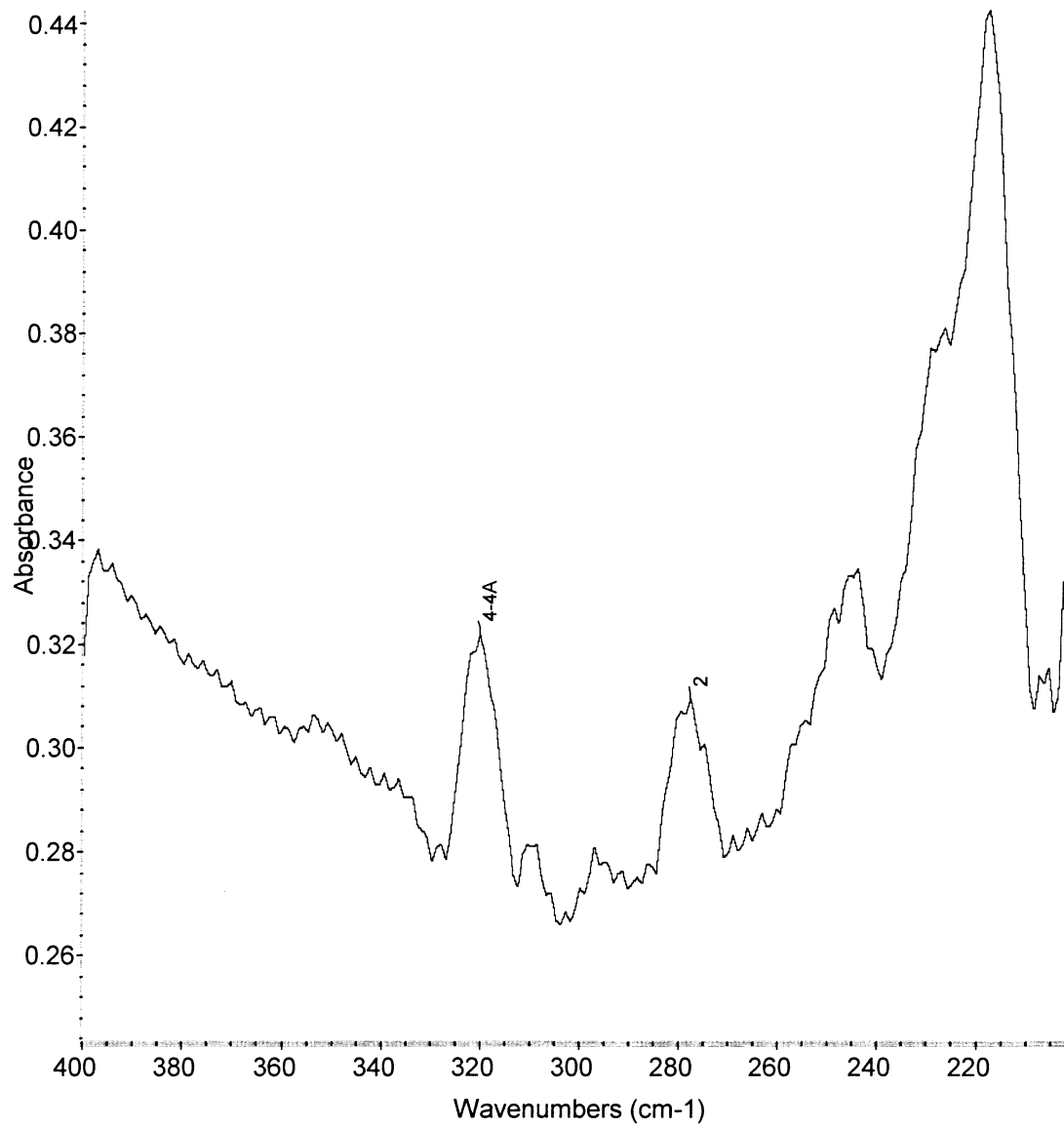


Figure 30: Spectrum for sample 1 of wafer 2, trial 2. Measurements were done at liquid helium temperature. The lines marked are boron excitation lines.

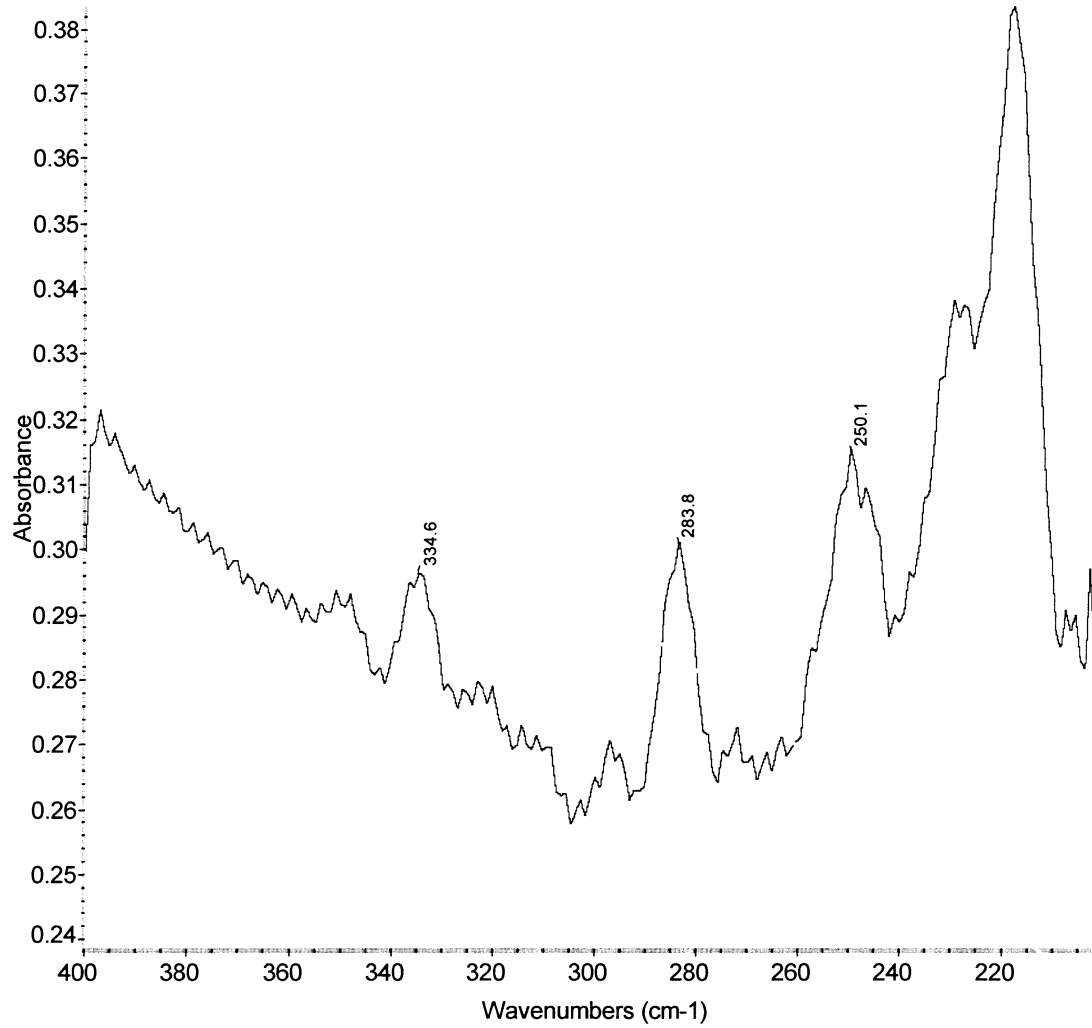


Figure 31: Spectrum for sample 2 of wafer 2, trial 1. Measurements were done at liquid helium temperature.

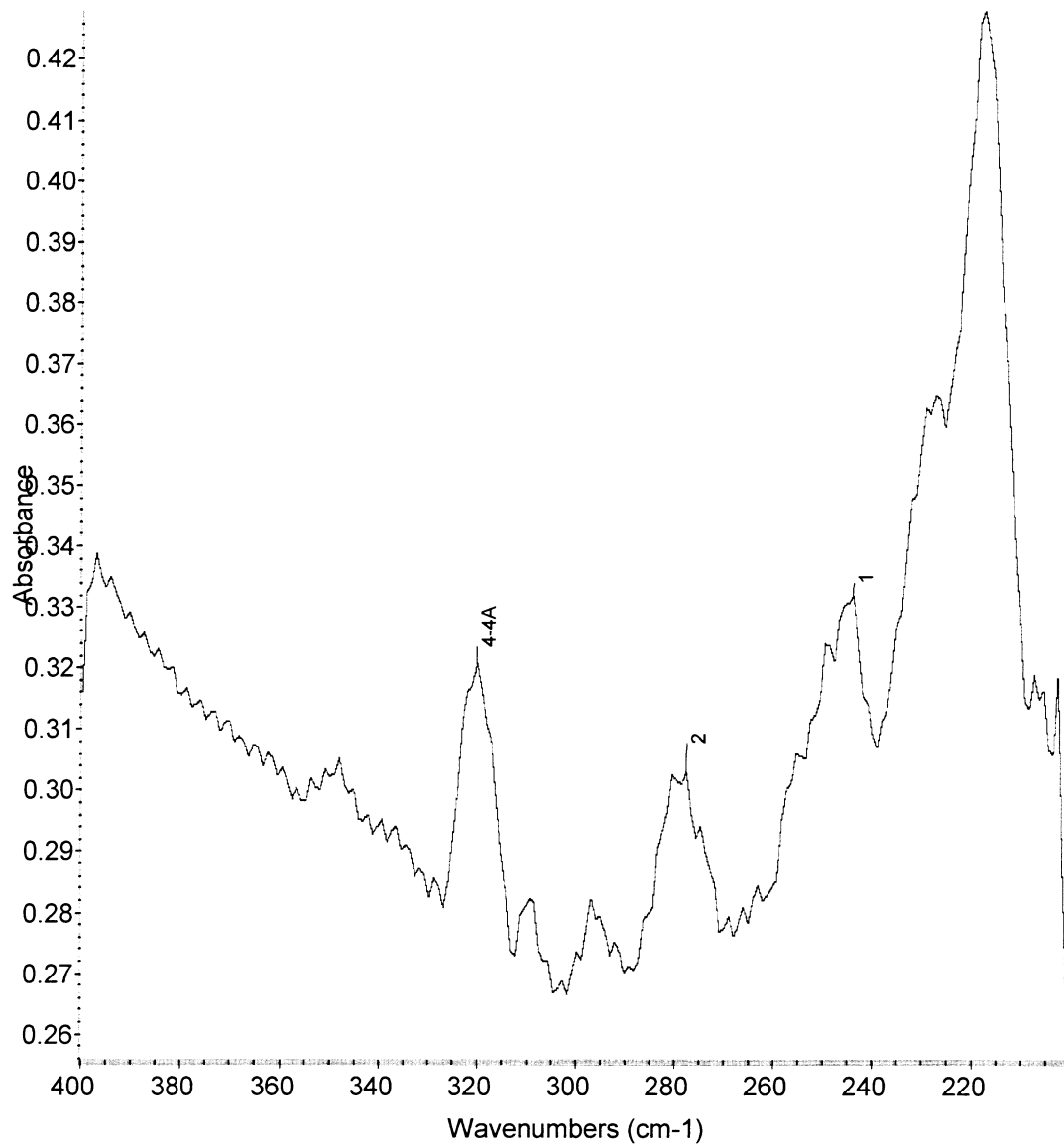


Figure 32: Spectrum for sample 2 of wafer 2, trial 2. Measurements were done at liquid helium temperature. The lines marked are boron excitation lines.

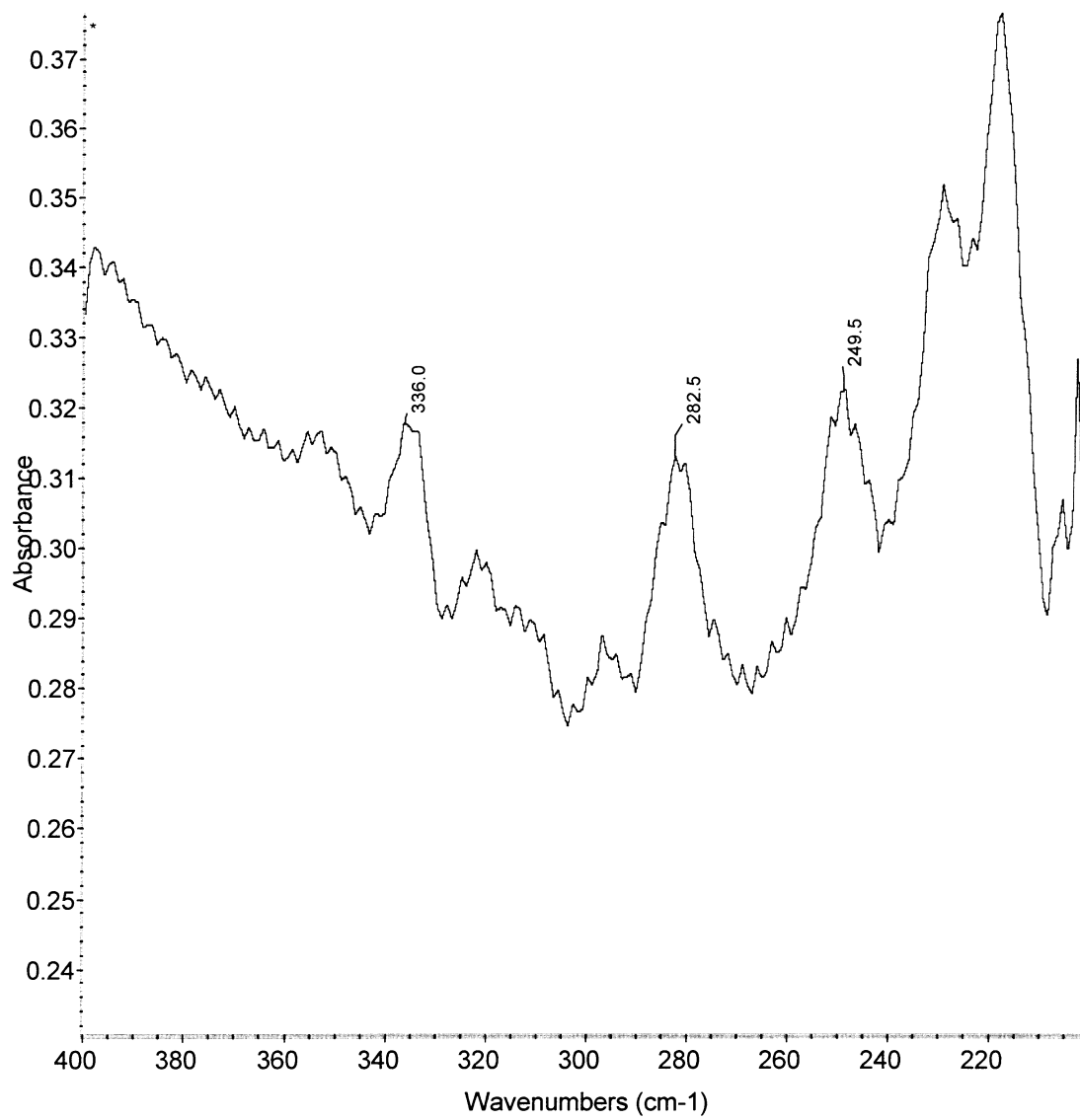


Figure 33: Spectrum for sample 3 of wafer 2, trial 1. Measurements were done at liquid helium temperature.

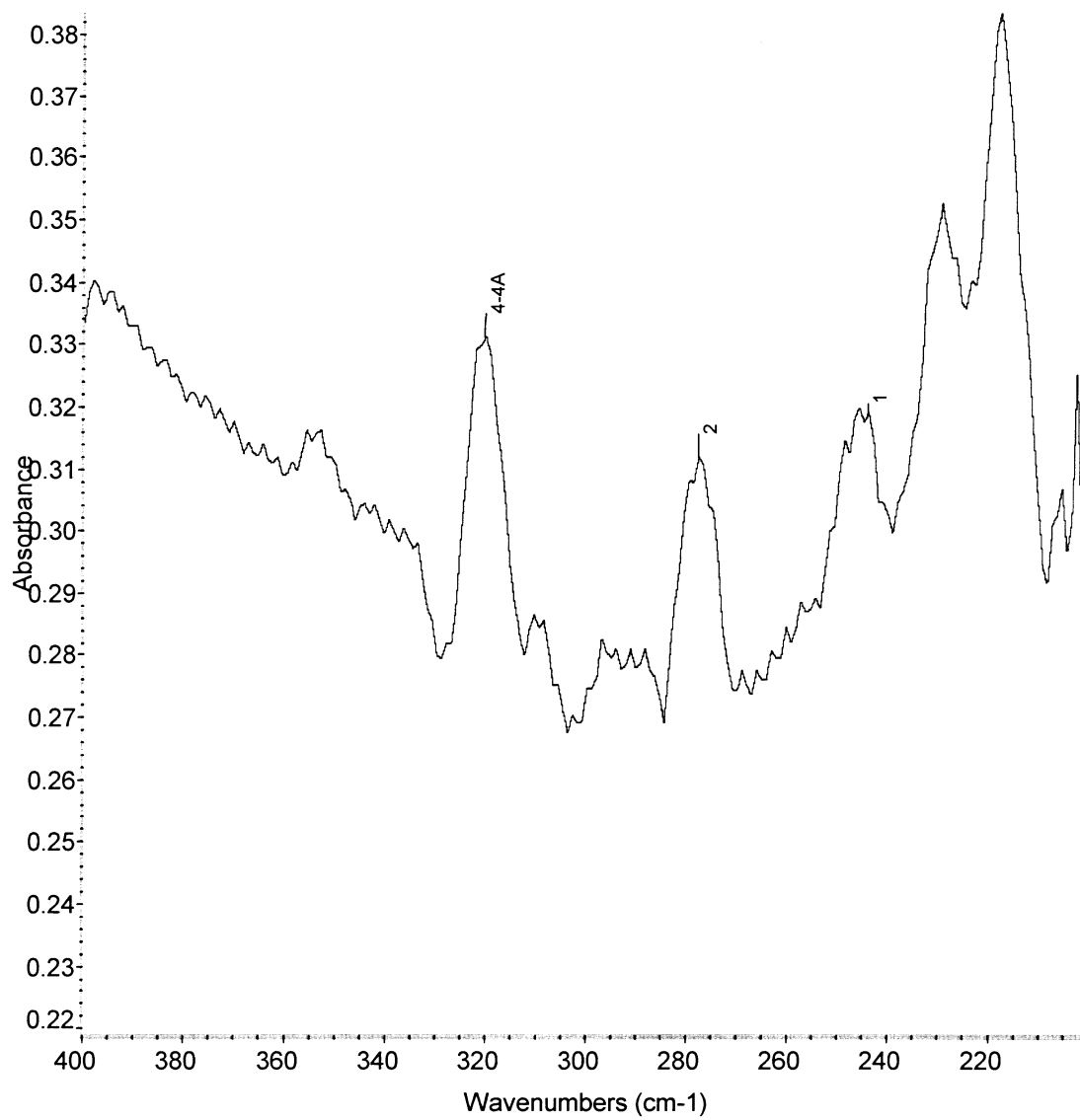


Figure 34: Spectrum for sample 3 of wafer 2, trial 2. Measurements were done at liquid helium temperature. The lines marked are boron excitation lines.

## CHAPTER V

### CONCLUSIONS AND RECOMMENDATIONS

#### Introduction

This chapter gives the conclusions from the experiments that were conducted and recommendations for further research.

#### Conclusions

The results obtained in the research show that subjecting a 4 inch wafer to single laser pulses at the corners of square of side 2 inches does not anneal the whole wafer. The spectra obtained show that boron had been annealed in the six samples that were analyzed. It is not clear whether this could be due to the laser pulses or the boron had undergone annealing during the process of growing the ingots from which the wafers were cut or some other processing stage. If this was due to the laser then this would raise the question as to why phosphorus was not annealed. This could be a subject for future research. The use of a control sample would help to resolve this issue.

### Recommendations for Further Research

In order to obtain data which is more representative of the whole wafer it might be a good idea to divide the wafer into a grid and take samples in a systematic manner across the whole wafer. This approach might give a better idea of the extent to which the wafer as a whole was annealed. In this research three samples were analyzed from each wafer. Increasing the number of samples would obviously result in more information on the extent to which the wafer was annealed.

As indicated earlier, it might be important to include some control samples which are not subjected to laser pulses as well as those which are annealed thermally. This would help in the interpretation of the data that is collected in the research.

## REFERENCES

Campbell, Stephen A. 2008. *Fabrication Engineering at the Micro- and Nanoscale*. New York: Oxford University Press.

Donnelly, D. W., B. C. Covington, J. Grun, C. A. Hoffman, J. R. Meyer, C. K. Manka, O. Glembocki, S. B. Qadri, and E. F. Skelton. 1997. Far-infrared spectroscopic, magnetotransport, and x-ray study of athermal annealing in transmutation-doped silicon. *Appl. Phys. Lett.* **71**: no. 5

Donnelly, D. W., B. C. Covington, J. Grun, R. P. Fischer, M. Peckerar, and C. L. Felix. 2001. Athermal annealing of low-energy boron implants in silicon. *Appl. Phys. Lett.* **78**: no. 14

Grun J., C. K. Manka, C. A. Hoffman, J. R. Meyer, O. J. Glembocki, R. Kaplan, S. B. Qadri, and E. F. Skelton. 1997. Athermal annealing of silicon. *Phys. Rev. Lett.* **78**: 1584-1587.

- Grun J., R.P. Fischer, M. Peckerar, C. L. Felix, B. C. Covington, D. W. Donnelly, B. Boro Djordjevic, R. Mignogna, J. R. Meyer, A. Ting, and C. K. Manka. 2000a. Athermal Annealing of Silicon Implanted with Phosphorus and Arsenic. In Proceedings of the International Symposium: Rapid Thermal and Other Short-Time Processing Technologies. Vol 2000-9. Pennington: The Electrochemical Society.
- Grun J., R. P. Fischer, M. Peckerar, C. L. Felix, B. C. Covington, D. W. Donnelly, B. Boro Djordjevic, R. Mignogna, J. R. Meyer, A. Ting, and C. K. Manka. 2000b. *Appl. Phys. Lett.* Athermal annealing of phosphorus-ion-implanted silicon **77**: 1997-1999.
- Jaeger, Richard C. 2002. Introduction to Microelectronic Fabrication. Volume V. Upper Saddle River: Prentice Hall.
- Jagannath, C., Z. W. Grabowski, and A. K. Ramdas. 1981. Linewidths of the electronic excitation spectra of donors in silicon. *Phys. Rev. B.* **23**: 2082-2098.
- Kittel, Charles. 1986. Introduction to Solid State Physics. New York: John Wiley and Sons.
- Kittel C., and A. H. Mitchell. 1954. Theory of donor and acceptor states in silicon and germanium. *Phys. Rev.* **96**: 1488-1493.
- Kohn W. 1957a. Shallow impurity states in silicon and Germanium. Vol. 5 of Solid State Physics. New York: Academic Press.

Kohn W. 1957b. Effective mass theory in solids from a many-particle standpoint. *Phys. Rev.* **105**: 509-516.

Kohn W., and J. M. Luttinger. 1955. Theory of donor states in silicon. *Phys. Rev.* **98**: 915-922.

Long, Donald, and John Myers. 1959. Hall effect and impurity levels in phosphorus-doped silicon. *Phys. Rev.* **115**: 1119-1121.

Lynch, S. A., G. Matmon, S. G. Pavlov, K. L. Litvinenko, B. Redlich, A. F. G. Van der Meer, N. V. Abrosimov, and H. W. Huberts. 2010. Inhomogeneous broadening of phosphorus donor lines in far-infrared spectra of single-crystalline SiGe. *Phys. Rev. B* **82**: 245206-1 – 245206-7.

Mahan, Gerald D. 2009. Quantum Mechanics in a Nutshell. Princeton University Press: Princeton.

Mayur, A. J., M. Dean Sciacca, A. K. Ramdas, and S. Rodriguez. 1993. Redetermination of the valley-orbit (chemical) splitting of the 1s ground state of group-V donors in silicon. *Phys. Rev. B.* **48**: 10893-10898.

Omar, Ali M. 1993. Elementary Solid State Physics. Boston: Addison-Wesley.

Pajot, Bernard and Dominique Debarre. 1981. Quantitative determination of B and P in silicon by IR Spectroscopy. In Neutron-Transmutation-Doped Silicon, ed. Jens Guldborg, 423-435. New York: Plenum Press.

- Pankove, Jacques I. 1975. *Optical Processes in Semiconductors*. New York: Dover Publications.
- Pearson, G. L., and J. Barden. 1948. Electrical Properties of Pure Silicon and Silicon Alloys Containing Boron and Phosphorus. *Phys. Rev.* **75**: 865-883.
- Ramdass, A K., and S. Rodriguez. 1981. Spectroscopy of the solid-state analogues of the hydrogen atom: donors and acceptors in semiconductors. *Rep. Prog. Phys.* **44**: 1297-1387.
- Scroder, Dieter K. 1998. *Semiconductor Material and Device Characterization*. New York: John Wiley and Sons.
- Shen, S. C., and M. Cardona. 1981. Infrared and far-infrared absorption of B- and P—doped amorphous Si. *Phys. Rev. B* **23**, 5322-5328.
- Streetman, Ben G., and Sanjay Banerjee. 2002. *Solid State Physics*. Upper Saddle River: Prentice Hall.
- Sze, S. M. 2002. *Semiconductor Devices. Physics and Technology*. Hoboken: John Wiley and Sons.
- Wilson J., and J. F. B. Hawkes. 1989. *Optoelectronics: an introduction*. London: Prentice Hall.
- Winkler Roland. 2003. *Spin-Orbit Coupling Effects in Two-Dimensional Electron and Hole Systems*. Berlin: Springer-Verlag.

## VITA

Dominic graduated from high school in 1989 and enrolled at the University of Zimbabwe to study for a Bachelor of Science degree in Mathematics and Physics. After graduating in 1992, he worked as a high school Physics teacher. In 1997 he went back to the University of Zimbabwe to study for a special honors degree in Physics. After completing the honors degree he enrolled for a master's degree in Agricultural Meteorology at the same institution. After completing the master's degree he got a lectureship post at Midlands State University. He worked at that institution until the end of 2008 when he came to the United States to study for a master's degree in Materials Physics.

Permanent Address: [dfchiroro@yahoo.com](mailto:dfchiroro@yahoo.com)

This thesis was typed by Dominic Chiroro.